

Rhesus_NVX-CoV2373_rev59-AG

2 February 2021

1 *Research Article*

2
3 **Title:** Collaboration between the Fab and Fc contribute to maximal protection against SARS-
4 CoV-2 in nonhuman primates following NVX-CoV2373 subunit vaccine with Matrix-M™ vaccination

5
6 **Authors:** Matthew J Gorman^{1#}, Nita Patel^{2#}, Mimi Guebre-Xabier^{2#}, Alex Zhu^{1#}, Caroline
7 Atyeo^{1#}, Krista M. Pullen^{3#}, Carolin Loos^{1,3#}, Yenny Goez-Gazi⁴, Ricardo Carrion Jr⁴, Jing-Hui
8 Tian², Dansu Yaun¹, Kathryn Bowman¹, Bin Zhou², Sonia Maciejewski², Marisa E. McGrath⁵,
9 James Logue⁵, Matthew B. Frieman⁵, David Montefiori⁶, Colin Mann⁷, Sharon Schendel⁷,
10 Fatima Amanat⁸, Florian Krammer⁸, Erica Ollmann Saphire⁷, Douglas Lauffenburger³, Ann M.
11 Greene², Alyse D. Portnoff², Michael J. Massare², Larry Ellingsworth², Gregory Glenn², Gale
12 Smith^{2*} and Galit Alter^{1*}

13
14 **Affiliations:**

15
16 ¹Ragon Institute of MGH, MIT, and Harvard, Cambridge, MA 02139, USA.

17 ²Novavax, Inc., 21 Firstfield Road, Gaithersburg, MD 20878, USA.

18 ³Department of Biological Engineering, Massachusetts Institute of Technology, Cambridge, MA
19 02139, USA

20 ⁴Texas Biomedical Research Institute. 8715 West Military Drive, San Antonio, TX 78227, USA.

21 ⁵University of Maryland, School of Medicine, 685 West Baltimore St, Baltimore, MD 21201,
22 USA.

23 ⁶Department of Surgery, Duke University Medical Center, Durham, NC 27710, USA

24 ⁷La Jolla Institute for Immunology, La Jolla, CA 92037, USA.

25 ⁸Department of Microbiology, Icahn School of Medicine at Mount Sinai, New York, NY, USA.

26
27 # These authors contributed equally.

28 * Co-corresponding authors: Gale Smith: gsmith@novavax.com and Galit Alter:
29 galter@mg.harvard.edu

30
31 **Highlights**

- 32 • NVX-CoV2373 subunit vaccine elicits receptor blocking, virus neutralizing antibodies, and
33 Fc-effector functional antibodies.
- 34 • The vaccine protects against respiratory tract infection and virus shedding in non-human
35 primates (NHPs).
- 36 • Both neutralizing and Fc-effector functions contribute to protection, potentially through
37 different mechanisms in the upper and lower respiratory tract.
- 38 • Both macaque and human vaccine-induced antibodies exhibit altered Fc-receptor binding to
39 emerging mutants.

Rhesus_NVX-CoV2373_rev59-AG

2 February 2021

40 **Abstract**

41 Recently approved vaccines have already shown remarkable protection in limiting SARS-CoV-2
42 associated disease. However, immunologic mechanism(s) of protection, as well as how boosting alters
43 immunity to wildtype and newly emerging strains, remain incompletely understood. Here we deeply
44 profiled the humoral immune response in a cohort of non-human primates immunized with a stable
45 recombinant full-length SARS-CoV-2 spike (S) glycoprotein (NVX-CoV2373) at two dose levels,
46 administered as a single or two-dose regimen with a saponin-based adjuvant Matrix-M™. While antigen
47 dose had some effect on Fc-effector profiles, both antigen dose and boosting significantly altered overall
48 titers, neutralization and Fc-effector profiles, driving unique vaccine-induced antibody fingerprints.
49 Combined differences in antibody effector functions and neutralization were strongly associated with
50 distinct levels of protection in the upper and lower respiratory tract, pointing to the presence of combined,
51 but distinct, compartment-specific neutralization and Fc-mechanisms as key determinants of protective
52 immunity against infection. Moreover, NVX-CoV2373 elicited antibodies functionally target emerging
53 SARS-CoV-2 variants, collectively pointing to the critical collaborative role for Fab and Fc in driving
54 maximal protection against SARS-CoV-2. Collectively, the data presented here suggest that a single dose
55 may prevent disease, but that two doses may be essential to block further transmission of SARS-CoV-2
56 and emerging variants.

57
58 **Key words:** NVX-CoV2373 vaccine, Matrix-M™ adjuvant, SARS-CoV-2 spike glycoprotein,
59 non-human primate, COVID-19.

Rhesus_NVX-CoV2373_rev59-AG

2 February 2021

60 **Introduction**

61 SARS-CoV-2 causes a spectrum of respiratory disease from asymptomatic to mild and severe
62 coronavirus disease (COVID-19). Since it crossed into humans, the virus has spread globally
63 with over 90 million confirmed cases and over 2 million deaths¹. COVID-19 manifests with a
64 range of clinical symptoms from asymptomatic to severe disease, with 50-75% of infected
65 individuals exhibiting asymptomatic infection and only a small proportion (2-5%) developing
66 severe disease, requiring mechanical ventilation²⁻⁴. The vaccines authorized for emergency use,
67 mRNA-1273 and BNT162b2, have been successful in preventing severe infections and inducing
68 anti-SARS-CoV-2 CD4⁺ T cell, CD8⁺ T cell, and potent neutralizing antibody responses⁵⁻⁷.
69 However, whether these vaccines confer protection against transmission as well as disease
70 remains unclear.

71
72 Emerging Phase 3 data suggest that vaccine-mediated protection emerges as early as 10 days
73 following primary vaccination^{8,9}, at a time when neutralizing antibodies are low or undetectable⁵⁻
74 ⁷. Similarly, emerging correlates of immunity following administration of DNA- and adenoviral-
75 vector SARS-CoV-2 vaccination point to a potential additional role for added antibody effector
76 functions, in collaboration with neutralization, as key correlates of immunity against SARS-
77 CoV-2^{10,11}. However, whether these responses evolve following the prime or the boost, provide
78 differential protection across the upper and lower respiratory tract, and provide protection against
79 variants remains unclear.

80
81 In this study, we deeply interrogated humoral correlates of protection in a cohort of rhesus
82 macaques immunized with one or two doses 5 or 25 μ g of a stabilized recombinant full-length
83 SARS-CoV-2 spike (S) glycoprotein (NVX-CoV2373) with 50 μ g Matrix-M adjuvant. Animals
84 immunized with the two-dose regimen, regardless if given the high (25 μ g) or low (5 μ g) antigen
85 dose, were protected against upper and lower respiratory infection (URTI and LRTI) and
86 shedding of replicating virus, while a single vaccine injection (regardless of antigen dose) was
87 only partially protective against infection. Distinct combinations of Fc-features and neutralizing
88 antibody responses were associated with protection in the upper and lower respiratory tract,
89 pointing to potential mechanistic differences required to control the virus at these distinct
90 immunological locations. Critically, the NVX-CoV2373 generated binding and functional

Rhesus_NVX-CoV2373_rev59-AG

2 February 2021

91 humoral immune responses to several emerging SARS-CoV-2 variants. These data point to
92 boosting-driven functional maturation of the humoral immune response as a key immune event
93 required to achieve full protection against infection and transmission of SARS-CoV-2 and
94 emerging mutants.

95

Rhesus_NVX-CoV2373_rev59-AG

2 February 2021

96 **Results**

97 *Subgenomic virus mRNA in respiratory samples*

98 Emerging Phase 3 data from mRNA vaccine platforms suggest that vaccine-induced protection
99 against disease is observable as early as 10 days following vaccine priming, prior to the presence
100 of robust neutralizing antibody levels^{8,9}. However, whether these responses are associated with
101 complete sterilizing immunity remains unclear. To define the specific humoral profiles that track
102 with protective immunity against disease and infection, we profiled the humoral immune
103 response induced by a stabilized, full-length SARS-CoV-2 Spike (S) vaccine (NVX-CoV2373)
104 following a prime-only or prime/boost vaccine regimen administered at 2 different antigen doses
105 (5 and 25 μ g) with Matrix-M adjuvant (50 μ g). Groups of rhesus macaques (n=5) were immunized
106 with one vaccine dose (study day 0) or two vaccine doses, spaced 3 weeks apart (study day 0 and
107 21). Control animals (n=4) received one or two injections of formulation buffer (placebo). Serum
108 was collected prior to immunization (day 0) and 21 and 31/32 days after the first dose (**Fig 1A**).

109
110 Protection was assessed by analyzing viral loads across the upper (nasal washes and nasal
111 pharyngeal swabs) and lower (bronchoalveolar lavage; BAL) respiratory tract on days 2-8 post-
112 infection (dpi). The highest levels of viral subgenomic RNA (sgRNA) were observed in placebo
113 animals across the upper and lower-respiratory tract samples, with peak viral loads observed 2dpi
114 and persistent sgRNA until day 7/8 (**Fig 1B, C, D**). Animals immunized with a single dose of
115 5 μ g or 25 μ g NVX-CoV2373 had lower levels of replicating virus at day 2 in all tissues
116 compared to placebo, however the 25 μ g dose was able to clear sgRNA in BAL and nasal
117 pharyngeal swabs at day 7/8, while the 5 μ g only cleared BAL. The animals that received 5 μ g or
118 25 μ g antigen in a prime/boost regimen had no detectable viral loads in BAL or nasal pharyngeal
119 swabs at any day and all sgRNA was cleared in nasal washes by day 4. In addition, tissue
120 samples were collected from the upper, middle, and lower right lung lobes; trachea; and nasal
121 cavity at the scheduled necropsy (7-8 dpi) and analyzed for viral gRNA. There was no gRNA in
122 nasal cavity, trachea, or lungs of animals immunized with 5 μ g or 25 μ g antigen in a prime/boost
123 regimen (**Fig 1E, F, G**). Conversely, nearly all placebo animals exhibited gRNA in each tissue
124 (**Fig 1E, F, G**). Animals immunized with a single vaccine dose were partially protected, with a
125 minority of animals having detectable gRNA. These data suggest that one vaccine dose was able
126 to induce a partially protective immune response, differing by antigen dose level, but two

Rhesus_NVX-CoV2373_rev59-AG

2 February 2021

127 vaccine doses resulted in full protection against infection along the respiratory tract, independent
128 of antigen dose.

129

130 *Antibody responses after NVX-CoV2373 immunization*

131 To determine if the humoral immune response could distinguish protected from non-protected
132 animals, we analyzed the IgG titers and neutralizing antibody response across the vaccine
133 groups. Robust anti-S IgG titers were observed across both vaccine groups after a single
134 immunization. Anti-S IgG titers remained stable at 31/32 days after 1 dose, however anti-S IgG
135 titers significantly increased 21-35-fold within 10 days following the booster immunization with
136 5 μ g or 25 μ g of NVX-CoV2373 (**Fig 2A**). Low levels of mucosal anti-S IgG antibodies were
137 detected in the nasal washes and BAL aspirates collected 31/32 days after one immunization,
138 increasing 8-22-fold in nasal washes and BAL aspirates at 10 days following the booster
139 immunization (**Fig 2B, 2C**).

140

141 To further profile the functional potential of the vaccine induced antibodies, a spike-pseudotype
142 virus neutralization assay was used to assess the neutralizing capacity in serum of immunized
143 animals. Serum from animals immunized with 5 μ g or 25 μ g NVX-CoV2373 had similar
144 pseudovirus neutralizing titers (ID₅₀) after a single dose. Following the booster immunization,
145 pseudovirus neutralizing titers significantly increased, with no significant differences noted
146 between the antigen doses (**Fig 2D**). In addition, live wild type virus neutralization assays and
147 hACE2 inhibition exhibited similar trends, with detectable neutralization/inhibition at day 21 in
148 all regimens, with a significant increase after the second vaccine dose (**Fig 2E and 2F**). Overall,
149 these results indicate that NVX-CoV2373 administered as a prime/boost regimen elicited high
150 anti-S IgG titers, capable of blocking binding to the hACE2 receptor and neutralizing in vitro
151 infectivity of spike-pseudotyped virus and wild type SARS-CoV-2. All non-human primates
152 (NHPs) treated with one dose had similar neutralization titers, but only some were protected
153 from viral infection, suggesting that neutralization may not be sufficient to fully explain
154 complete protection from infection, particularly following a single vaccine dose.

155

156 *System serology profiling*

Rhesus_NVX-CoV2373_rev59-AG

2 February 2021

157 Natural SARS-CoV-2 infection is marked by a rapid rise of multiple antibody isotypes and
158 subclasses, each positioned to recruit a diverse set of antibody effector functions^{12,13}. Recent
159 studies have noted a significant correlation between antibody-effector function, rather than
160 neutralization, with natural resolution of infection in humans¹⁴. Thus, we next examined the
161 evolution of subclass, isotype, Fc-receptor, and Fc-effector function across doses and boosting
162 strategies (**Supplementary Fig 1**).

163
164 As expected, based on titers (**Fig 2**), luminex IgG1 levels were robustly induced following a
165 single vaccine dose, indistinguishably across antigen levels, with a 1.5-4-fold increase following
166 a boost (**Fig 3A**). Similarly, IgA were induced robustly to a maximal level after one 25 μ g dose,
167 but required boosting to reach maximal levels in the 5 μ g vaccine group (**Fig 3A**). Conversely, a
168 trend towards higher levels of IgM were noted in 5 μ g vaccine group following a single vaccine
169 dose, that declined with a boost and were largely lost in the 25 μ g dose group (**Fig 3A**), pointing
170 to enhanced class switching to more mature antibody subclasses with boosting and higher
171 antigen doses. These data point to the first differences across antigen-dosing group, highlighting
172 equivalent IgG and IgA selection across groups, but more aggressive switching of IgM, shifting
173 the polyclonal balance of the vaccine-specific antibody pool towards a more mature Fc-
174 functional profile.

175
176 Changes in polyclonal antibody profiles result in the potential formation of distinct swarms of
177 antibodies able to engage with a target pathogen, forming qualitatively distinct immune
178 complexes, that collectively shape the Fc-receptors (FcRs) bound on innate immune cells,
179 thereby driving distinct antibody effector functions¹⁵⁻¹⁸. Thus, to explore differences in
180 functionality across doses and boosting regimens, we next profiled differences in binding
181 profiles across rhesus Fc-receptors. Equivalent Fc γ RIIA-1 binding was observed across the 2
182 antigen doses after the prime, although there was a trend to a loss of binding at day 31/32 in the
183 5 μ g dosing group (**Fig 3B**). However, after a boost, Fc γ RIIA-1 binding antibodies increased by
184 4-100-fold across the doses, with a trend towards higher binding antibodies in the 25 μ g dosing
185 group (**Fig 3B**). Nearly identical profiles were observed across the other rhesus FcRs, pointing to
186 a substantial quantitative advantage induced by the boost, that tended to differ across the doses.

187

Rhesus_NVX-CoV2373_rev59-AG

2 February 2021

188 Finally, to explore the functional impact of these changes in vaccine induced antibody Fc-
189 profiles, we examined the ability of the humoral response to stimulate antibody-dependent
190 functions: cellular monocyte phagocytosis (ADCP), neutrophil phagocytosis (ADNP),
191 complement deposition (ADCD), and NK degranulation (NKdegran). Similar ADCP responses
192 were induced across the antigen doses following a single vaccination (**Fig 3C**). Conversely,
193 robust augmentation of ADCP was observed with a boost (**Fig 3C**), that surprisingly tended to be
194 higher in the 5 μ g group. An identical profile was observed for NK-cell activating antibodies.
195 Neutrophil phagocytosis was slightly higher in the 5 μ g group after the prime, and then fully
196 matured across both groups with a boost, remaining slightly elevated in the 5 μ g group.
197 Conversely, complement activating antibodies were induced equivalently across the antigen-
198 dosing groups following a single dose, and increased with a boost in an antigen dose-
199 independent manner. Thus, while titers and neutralization reached near maximal potential after a
200 single vaccine dose, these data point to a critical role for boosting in driving the full maturation
201 of the Fc-effector potential of the vaccine induced humoral response, that are further subtly tuned
202 by antigen dosing.

203

204 *Unique humoral profiles of vaccine regimen*

205 Given the various univariate profile differences noted across the vaccine groups, we next aimed
206 to define whether distinct multivariate profiles were induced across the regimens. Aggregate data
207 clearly highlighted the striking influence of the boost and the more nuanced effects of antigen
208 dose on shaping the polyclonal vaccine response (**Fig 4A**). Antigen-dose effects emerged upon
209 unsupervised analysis using a principal component analysis (PCA), pointing to a tendency
210 towards separation between antigen dose and vaccine-specific antibody profiles in the animals
211 that received a single dose (**Fig 4B**), that was largely lost with the boost (**Fig 4C**). However,
212 integration of the 4 groups clearly demonstrated the dominant influence of the boost in shaping
213 antibody profiles(**Fig 4D**). Specifically, robust separation in antibody profiles across single and
214 double immunized animal vaccine-specific antibody profiles (**Fig 4D**), with a more subtle effect
215 of dose on shaping vaccine-specific antibody profiles, solely observed in the single dose arms.
216 Finally, radar plots of the humoral immune response across vaccine arms demonstrated the clear
217 explosion of humoral immune maturation with the second dose, albeit slight differences in
218 antibody effector functions were noted across the doses. Additionally, more nuanced differences

Rhesus_NVX-CoV2373_rev59-AG

2 February 2021

219 were observed in the single dose arms, with a more balanced functional response observed in the
220 25 μ g group compared to the 5 μ g immunized animals at day 31-32, prior to challenge (**Fig 4E**).
221 These data provide a deep immunologic view of the vaccine-induced polyclonal functional
222 profiles induced following vaccination, and how they are shaped by dose and boosting prior to
223 challenge.

224

225 *Immune correlates of protection from viral infection*

226 While neutralizing antibodies have been clearly linked to vaccine-mediated protection following
227 DNA¹¹, AD26¹⁰, protein¹⁹, and mRNA based vaccination⁵⁻⁷, protection has been noted in
228 humans prior to the evolution of neutralizing antibodies^{8,9}. Similarly, despite robust induction of
229 neutralizing antibodies given one or two doses of NVX-CoV2373, variable levels of protection
230 were observed against upper and lower respiratory viral loads across the groups (**Fig**
231 **1B,C,D,E,F,G**). To define the humoral correlates of immunity of viral control across the
232 respiratory tract, all antibody metrics were integrated, and an unsupervised multivariate analysis
233 was performed to objectively define antibody correlates of immunity. Clear separation was noted
234 in vaccine-induced antibody profiles across NHPs exhibiting complete protection against SARS-
235 CoV-2 compared to animals that exhibited viral loads in one or several compartments (**Fig 5A**).
236 Specifically, the PCA illustrated a substantial split in antibody profiles in animals that exhibited
237 no protection/protection in the lower respiratory tract (BAL) from animals that exhibited more
238 complete protection across the upper and lower-respiratory tract (nasal washes, nasal swabs, and
239 BAL). Thus, unsupervised analysis suggested the presence of unique humoral immune correlates
240 of immunity in lower and upper respiratory tracts.

241

242 To gain deeper resolution into the specific features of the humoral immune response that may
243 lead to these distinct levels of viral restriction across compartments, the relationship of individual
244 features and protection was assessed by calculating the area-under-the-curve for each receiver
245 operator characteristic (ROC) curve within each compartment (**Fig 5B**). The top features
246 associated with protection in the lower respiratory tract (BAL) included antibody titers, S2- and
247 S1-specific FcR binding, and hACE2 receptor inhibition. Similarly, the top features associated
248 with protection in the BAL and nasal pharyngeal swab included the levels of S1-specific
249 antibody titers of several IgG subclasses and hACE2 inhibition. However, complete protection

Rhesus_NVX-CoV2373_rev59-AG

2 February 2021

250 from viral replication across the upper and lower respiratory tracts was associated with a robust
251 whole S-specific multi-subclass specific response, complement-depositing functions, and
252 neutralizing antibody titers. The radar plots further illustrated the magnitude and multivariate
253 nature of the protective humoral immune response, marked by poor antibody responses in
254 unprotected animals, an expansion of subclasses, but not functions, in animals with solely lower
255 respiratory tract protection (BAL), an expanded functional and FcR-binding antibody profiles in
256 animals with BAL and nasal swab protection. Conversely, the largest, functionally expanded
257 humoral immune response was observed in animals with complete protection across the upper
258 and lower respiratory tract (**Fig 5C**). These data point to an intimate collaboration between the
259 Fc and Fab in driving full viral protection, where neutralization may be key to lower-respiratory
260 protection, but the potential need for additional Fc-effector functions in collaboration with
261 neutralization may be key for full protection across the respiratory tract.

262

263 *Antibody response to emerging SARS-CoV-2 mutants*

264 Despite the promising results observed in Phase 3 trials with the mRNA vaccines, significant
265 concern has recently arisen globally, due to the rapid emergence of SARS-CoV-2 variants across
266 the globe²⁰⁻²³. Among the variants, the recently identified genetic variant, B.1.1.7 (Public Health
267 England Variant of Concern) and B.1.351/501Y.V2 (South African Variant of Concern) include
268 multiple mutations in the Spike protein that appear to improve viral infectivity²⁴⁻²⁶ or escape
269 neutralizing antibodies^{27,28}. While early data suggested limited impact of the 501Y mutation on
270 neutralizing antibody responses²⁹⁻³¹, recent data suggest that this mutation may reduce mRNA
271 vaccine induced neutralization²⁷, matching recent Novavax vaccine efficacy results in the
272 UK^{32,33}. Conversely, consistently reduced neutralization has been noted against the emerging
273 viral variant from South Africa, in parallel to reduced vaccine efficacy in RSA^{27,32}. Yet, how
274 these mutations affect overall vaccine-induced immunity remains unclear. Thus, we profiled the
275 functional antibody response to the UK (B.1.1.7 RBD and N501YΔ69-70 Spike) and RSA
276 (B.1.351 RBD, E484K RBD and E484K Spike) variants compared to the D614G viral variant for
277 spike and WT variant for RBD. Strong correlations were observed between the dominant D614G
278 variant and the two emerging variant viruses, across all antibody metrics (**Fig 6A**). However,
279 some diminution of antibody binding (IgG1/IgG3) and Fc-receptor binding was noted across
280 both strains, albeit the effect was most pronounced for the RSA strains in both the macaques (**Fig**

Rhesus_NVX-CoV2373_rev59-AG

2 February 2021

281 **6A)** and humans (**Fig 6B**). Interestingly, macaques (**Fig 6A**) displayed a more pronounced loss
282 of humoral reactivity to the B.1.1.7 and B.1.351 variants compared to humans (**Fig 6B**), where
283 humans with high antibody titers largely retained FcR-binding to the mutants. Conversely,
284 human vaccinees with intermediate antibody titers exhibited a more profound loss of S-specific
285 FcR binding, potentially contributing to the observed vulnerability in a fraction of vaccinees to
286 infection/disease. Multivariate analyses by PCA, where variation in antibody profiles across
287 SARS-CoV-2 variants were captured (**Fig 6C**), point to altered binding, specifically in the
288 macaque humoral immune response across the E484K and B.1.351 RBD variants compared to
289 the UK variant. These data highlight the dominant effect of E484K in knocking out Fc-effector
290 function against the RBD, in addition to a loss of neutralization^{27-29,34} (**Supplementary Fig 2A-**
291 **C**).

292

293 These data point to a slight reduction in antibody effector function against the B.1.1.7
294 variants, but a diminished overall response to the E484K and B.1.351 variant that may explain
295 differences in the level of efficacy observed in the recent clinical trials³². The presence of more
296 robust recognition of the full Spike variants among individuals with robust humoral immune
297 responses, representing approximately half of the vaccinees, suggests that at high antibody titers,
298 vaccine induced immunity may contribute to protection against variants, via non-RBD specific
299 responses, the latter that are lost with the E484K mutation. Thus, these data suggest that NVX-
300 CoV2373 stimulates a robust humoral immune response that is fully functionally matured with
301 boosting. While antigen dose has a more limited influence on shaping the functional protective
302 profile of the humoral immune response, the induction of both neutralization and Fc-receptor
303 mediated activity represents key correlates of immunity against upper and lower respiratory tract
304 protection against SARS-CoV-2 and its variants, that may be key to both protection from disease
305 and transmission.

306

307 **Discussion**

308 Vaccine shortages, the need for rapid global deployment, increasing reinfection cases, and the
309 emergence of viral variants have collectively pointed to the urgent need to define correlates of
310 immunity against SARS-CoV-2 and its variants. Using a unique vaccine study, poised to profile
311 both the importance of antigen-dose and boosting, here we deeply and comprehensively

Rhesus_NVX-CoV2373_rev59-AG

2 February 2021

312 dissected the key correlates of immunity against upper and lower respiratory tract infection.
313 Despite the induction of robust vaccine-specific antibody titers and neutralization with a single
314 dose or two doses of 5 μ g or 25 μ g NVX-CoV2373, differential levels of viral restriction were
315 observed across animals in the upper and lower respiratory tracts. Specifically, animals receiving
316 a single dose vaccine were only partially protected against replicating virus in the upper
317 respiratory tract, whereas animals receiving 2 doses exhibited near complete protection. These
318 data suggest that a single dose may prevent disease, but that two doses may be essential to block
319 further transmission.

320

321 The improved protection of the two-dose vaccine was linked to a dramatic maturation of the Fc-
322 effector profiles of vaccine induced antibodies, that collaborated with neutralization as key
323 correlates of immunity against viral replication, with highly functional and neutralizing antibody
324 responses conferring the most robust restriction across the upper and lower respiratory tract.
325 Thus overall, these data demonstrate the critical importance of a coordinated Fab- and Fc-
326 mediated antibody response for full protection against SARS-CoV-2 infection, that may also
327 function against emerging variants.

328

329 Both human vaccines, mRNA-1273 and BNT162b2, require a prime and boost to achieve
330 optimal protection. However, as the logistical challenges become apparent in distributing a
331 vaccine globally, interest in increasing the available vaccine by reducing the amount of vaccine
332 or doses given per individual has increased. Preliminary retrospective analysis of the first dose of
333 the Pfizer/BNT162b2 before boosting suggested approximately a 52% protection from severe
334 infection^{5,35}. However, whether a single dose can provide long-term protection remains unclear.
335 While immunogenicity and durability vary significantly across vaccine platforms^{5-7,10,11,19}, our
336 data demonstrate some level of protection against lower-respiratory infection after a single
337 vaccine. Yet single dose vaccine-maintained IgM, exhibited incomplete class switching, poor
338 mucosal antibody levels, and demonstrated incomplete functional effector and neutralizing
339 responses, albeit a more balanced response was noted at the higher (25 μ g) antigen dose.
340 However, after two doses, the explosion of antibody effector function and neutralization likely
341 resulted in a significant increase in protection against both upper and lower respiratory viral

Rhesus_NVX-CoV2373_rev59-AG

2 February 2021

342 replication, linked to the combined presence of potent neutralizing and Fc-effector inducing
343 antibodies and continue to point to the value of the booster immunization.

344

345 Neutralizing antibodies represent a critical obstacle to viral infection at the time of infection.
346 However, the density of antibody-producing cells likely varies along the respiratory tract, with a
347 higher density of immune cells found in the lower respiratory tract compared to the more
348 immune barren upper respiratory tract^{36,37}. Thus, to achieve complete sterilizing protection from
349 infection in the upper respiratory tract, it is plausible that additional immune mechanisms may be
350 required in the upper respiratory tract to compensate for potentially lower antibody levels. Here
351 we observed the key role of neutralizing antibodies deep within the lungs, but the critical
352 importance of SARS-CoV-2 antibodies of multiple subclasses, binding to multiple Fc-receptors,
353 and complement activation as key additional functional mechanisms that may contribute to upper
354 respiratory protection. Given that the NVX-CoV2373 vaccine induced potent neutralizing
355 antibodies across doses and regimens, we were unable to divorce the influence of neutralization
356 and Fc-effector function. Similar profiles have been noted following reinfection, DNA and
357 Ad26-vaccine studies, marking the co-evolution of the Fab and Fc, and the importance of both
358 ends of the molecule in protective immunity^{10,11}. However, whether neutralization and/or Fc-
359 effector function persist differentially over time following vaccination, conferring different
360 levels of protection may provide key insights on precise durable correlates of immunity.

361

362 As the virus has begun to adapt to populations across the globe, a number of SARS-CoV-2
363 variants have begun to emerge. The D641G mutation spread rapidly from Europe to other
364 continents, resulting in a conformational change in the rigidity of the RBD, resulting in enhanced
365 infectivity in vitro, but resulting in no escape from neutralizing antibodies³⁸⁻⁴³. Similarly, more
366 recently the B.1.1.7 mutation has spread across and out of the UK since September 2020²¹,
367 representing 3 key mutations N501Y, P681H, and Δ 69-70, that have been linked to enhanced
368 ACE2-binding, but limited impact on neutralizing antibody activity by monoclonal or the
369 Pfizer/BNT162b2^{20,26,28,30,31,44}. Additional variants have begun to emerge in South Africa
370 (B.1.351/501Y.V2) and Brazil (P.1), including mutations both in the RBD and the N-terminal
371 domain of the S-protein, demonstrating significant evasion of antibody-mediated
372 neutralization^{28,31,45-49}. Here we noted a loss of both binding and FcR binding activity across the

Rhesus_NVX-CoV2373_rev59-AG

2 February 2021

373 variants in both macaques and humans, with a more profound loss of binding to RSA variant
374 mutations, particularly related to a nearly complete loss of RSA RBD-specific humoral
375 immunity. However, full Spike-specific antibody binding persisted in approximately half of the
376 human vaccinees, particularly in those with robust antibody titers, pointing to the potential for
377 persisting Fc-effector functions as a key compensatory correlate of immunity in the face of
378 evolving mutants that knock out RBD-binding and neutralization. These data mirror the observed
379 rates of protection observed in the recent Phase2 vaccines studies³², further substantiating the
380 potential critical importance of both Fab and Fc-functionality in overall population level vaccine
381 efficacy. Yet, further research is needed promptly to identify the impact of emerging mutations
382 on both neutralization and other antibody effector functions that may contribute to antiviral
383 control and protection.

384

385 After just 4 months, the WHO declared that the SARS-CoV-2 virus had caused a worldwide
386 pandemic. In response, several vaccines have progressed through late stages of clinical
387 evaluation. To date, messenger RNA (mRNA) vaccines, BNT162b2 and mRNA-1273, recently
388 received Emergency Use Authorization (EUA). Although these vaccines have an acceptable
389 safety profile and effectively protect against more severe disease, they require freezing, have
390 limited data on long-term durability, and have not been shown to protect against infection or
391 transmission. Moreover, given the limited number of vaccine doses available, more vaccine
392 candidates are urgently needed that are able to counteract both wildtype and emerging variant
393 strains. Thus, the need to understand correlates of immunity has never been more urgent, to
394 support the selection and design of additional vaccines able to confer global protective immunity.
395 Here, we describe the identification of correlates of immunity using a subunit vaccine that is
396 stable at refrigerated temperatures, and is immunogenic and well tolerated in human studies¹⁹. In
397 this study, we demonstrate the presence of binding and neutralizing antibody titers after a single
398 immunization, using either 5 μ g or 25 μ g of vaccine, but a remarkable maturation of the Fc-
399 effector profile after a second immunization. Moreover, while partial protection was observed
400 with neutralizing antibodies alone after a single round of immunization, complete protection in
401 the upper and lower respiratory tract was observed with a second round of immunization,
402 marking critical Fab and Fc-mediated correlates of immunity that may be key to both protection
403 against disease and transmission of SARS-CoV-2 and emerging variants. Thus this work bolsters

Rhesus_NVX-CoV2373_rev59-AG

2 February 2021

404 the value of boosting, which will undoubtedly be critical not only to achieve complete protection
405 against infection and transmission, but also to drive durability. Collectively, these data provide
406 key insights into compartment specific immune correlates that may be critical for protection
407 against virus shedding that could help meet an urgent public health need and accelerate the
408 establishment of herd immunity^{50,51}.

409

410 **Materials and methods**

411 *Cell line, viruses, and receptor*

412 Vero E6 cells were obtained from ATCC, CRL-1586 and maintained in Minimal Eagles Medium
413 (MEM) supplemented with 10% fetal bovine serum (FBS), 1% glutamine, and 1% penicillin and
414 streptomycin (P/S). THP-1 cells (ATCC TIB-202) maintained in Roswell Park Memorial
415 Institute (RPMI) medium, supplemented with 10% FBS, 1% glutamine, 1% P/S, 1% HEPES, and
416 50 μ M β -ME. HEK 293T/ACE2 cells were obtained from Drs. Michael Farzan and Huihui Mu at
417 the Scripps Research Institute (Jupiter, FL, USA). For the challenge phase of the study, the
418 SARS-CoV-2 (USA-WA-1/2020) passage 4 (P4) isolate was obtained from Biodefense and
419 Emerging Infections Research Resource Repository (catalog number NR-52281, BEI Resources,
420 GenBank accession number MN985325.1). For the in vitro neutralization assay, the SARS-CoV-
421 2 (USA-WA-1/2020) isolate was obtained from the Center for Disease Control and provided by
422 Dr. Matthew Frieman, University of Maryland. Histidine-tagged human ACE2 receptor was
423 purchased from Sino Biologics (Beijing, CHN). Matrix-MTM adjuvant was provided by Novavax,
424 AB (lot number M1-111, Uppsala, SWE)⁵².

425

426 *NVX-CoV2373 spike glycoprotein*

427 The SARS-CoV-2 S vaccine was constructed from the full-length, wild-type SARS-CoV-2 S
428 glycoprotein based on the GenBank gene sequence MN908947 nucleotides 21563-25384. The
429 native S protein was modified by mutating the putative furin cleavage site (682-RRAR-685 to
430 682-QQAQ-685) in the S1/S2 cleavage domain to confer protease resistance. Two additional
431 proline amino acid substitutions were inserted at positions K986P and V987P (2P) within the
432 heptad repeat 1 (HR1) domain to stabilize SARS-CoV-2 S in a prefusion conformation⁵³. The
433 synthetic transgene was codon optimized and engineered into the baculovirus vector (BV2373)
434 for expression in *Spodoptera frugiperda* (Sf9) insect cells (GenScript, Piscataway, NJ, USA).

Rhesus_NVX-CoV2373_rev59-AG

2 February 2021

435 NVX-CoV2373 spike trimers were detergent extracted from the plasma membrane with
436 phosphate buffer containing TERGITOL NP-9, clarified by centrifugation, and purified by
437 TMAE anion exchange and lentil lectin affinity chromatography. Purified NVX-CoV2373 (547
438 $\mu\text{g mL}^{-1}$, lot number BV2373-16APR20) was formulated in 25 mM sodium phosphate (pH 7.2),
439 300 mM NaCl, and 0.02% (v/v) polysorbate and supplied frozen at $-80^{\circ}\text{C} \pm 10^{\circ}\text{C}^{54}$.

440

441 *Animal ethics statement*

442 The immunization and challenge phases of the study complied with all applicable sections of the
443 Final Rules of the Animal Welfare Act regulations (9 CFR Parts 1, 2, and 3) and *Guide for the*
444 *Care and Use of Laboratory Animals - National Academy Press, Washington D. C. 8th Edition,*
445 *2011 (The Guide)*. The study was conducted at the Texas Biomedical Research Institute (Texas
446 Biomed, San Antonio, TX, USA), an AAALAC (Association for the Assessment and
447 Accreditation of Laboratory Animal Care) accredited facility. The work was conducted in
448 accordance with a protocol approved by Texas Biomed's Institutional Animal Care and Use
449 Committee.

450

451 *Human ethics statement*

452 The Phase 1 vaccine study was previously described¹⁹. Healthy 18-59-year-old men and non-
453 pregnant women were included in the study. Previously infected individuals were excluded. With
454 the exception of 6 sentinel participants vaccinated in an open-label manner, the remaining 125
455 participants were randomly assigned to vaccine and placebo groups in a blinded fashion. All
456 subjects signed informed consent and safety oversight was monitored by a data monitoring
457 board.

458

459 *Animal husbandry*

460 Animals were housed individually in stainless steel cages with wire mesh bottoms. Animals were
461 fed commercially available certified primate diet from Purina Mills 5048 (LabDiet) and provided
462 water *ad libitum* from an institutional watering system that was analyzed monthly for impurities.
463 Environmental conditions included 12 hour light and 12 hour dark cycle with controlled
464 temperature ($74^{\circ}\text{F} \pm 10^{\circ}\text{F}$) and humidity (30% to 70% RH). Cages were cleaned daily.

465

Rhesus_NVX-CoV2373_rev59-AG

2 February 2021

466 Twenty-four experimentally naïve rhesus macaques (*Macaca mulatta*) of Chinese origin were
467 sourced from Envigo (Alice, TX, USA). Animals were screened and determined to be negative
468 for Simian Immunodeficiency Virus (SIV), Simian T-Lymphotropic Virus-1 (STLV-1), Simian
469 Varicella Virus (SVV) and *Macacine herpesvirus 1* (Herpes B virus), and Simian Retrovirus
470 (SRV1 and SRV2) by polymerase chain reaction (PCR), and negative for *Trypanosoma cruzi*.
471 Rectal swabs were collected and tested for Shigella, Campylobacter, Salmonella, and Yersinia.
472 Pharyngeal swabs were used to test for *Bordetella bronchiseptica*. All animals were tested and
473 verified to be negative for tuberculosis.

474

475 The vaccination phase of the study was performed in the Texas Biomed Animal Biosafety Level
476 2 (ABSL-2) facility. Following the immunization phase of the study, animals were transferred
477 and acclimated for 7 days in the Texas Biomed ABSL-3 facility prior to challenge. Animals were
478 monitored a minimum of twice daily for the duration of the study.

479

480 *Study blinding*

481 This study was blinded (assignment to vaccinated/immunized versus placebo group) to avoid
482 bias in evaluation, euthanasia, gross pathology assessment, and qRT-PCR assay outcome. All
483 staff performing in vitro assays were blinded to the animal vaccine dosage and to whether the
484 animal received vaccine or placebo while performing assays and analysis.

485

486 *Study design*

487 Animals were randomly assigned to groups, with stratification across age and gender, using a
488 computerized randomization procedure. Twenty-four (12 male and 12 female) rhesus macaques,
489 within the age range of >3 to <8-year-olds and weight range ≥ 3.67 kg to ≤ 10 kg, were
490 randomized into four immunization groups and two placebo groups. NVX-CoV2373 was
491 formulated with 50 μ g Matrix-M on the day of immunization. The placebo groups received
492 formulation buffer. Groups 1 (1 male and 1 female) received placebo in two doses spaced 21
493 days apart (study day 0 and 21) and group 4 (1 male and 1 female) received placebo in one dose
494 (study day 0). Group 2 (2 females and 3 males) received 5 μ g NVX-CoV2373 + 50 μ g Matrix-M
495 and group 3 (2 females and 3 males) received 25 μ g NVX-CoV2373 + 50 μ g Matrix-M in two
496 doses spaced 21 days apart (study day 0 and 21). Group 5 (3 females and 2 males) received 5 μ g

Rhesus_NVX-CoV2373_rev59-AG

2 February 2021

497 NVX-CoV2373 + 50 μ g Matrix-M and group 6 (3 females and 2 males) received 25 μ g NVX-
498 CoV2373 + 50 μ g Matrix-M in one dose (study day 0). Injections (0.5 mL) were administered in
499 the thigh muscle.

500

501 Animals were sedated by intramuscular (IM) administration of Telazol (2-8 mg kg⁻¹, IM) prior to
502 vaccination, collection of blood samples, virus challenge, collection of nasal swabs, nasal
503 washes, and bronchoalveolar lavage (BAL). For serologic assessments, serum was collected on
504 study day 0 prior to immunization and day 21, and day 31 or 32 after the first immunization and
505 stored at -80°C until assayed. Nasal washes, nasal pharyngeal swabs, and BAL were collected on
506 study day 31/32, prior to challenge.

507

508 *Anti-spike IgG and IgA ELISA*

509 Serum, nasal wash, and BAL anti-SARS-CoV-2 spike (S) protein IgG titers were determined by
510 ELISA. Briefly, 96-well plates (Thermo Fisher Scientific, Rochester, NY, USA) were coated
511 with 1.0 μ g mL⁻¹ of SARS-CoV-2 S protein (BV2373, Lot# 16Apr20, Novavax, Inc.
512 Gaithersburg, MD, USA). Plates were washed with phosphate buffered Tween (PBS-T) and non-
513 specific binding was blocked with TBS Startblock blocking buffer (Thermo Fisher Scientific,
514 Rochester, NY, USA). Serum samples were serially diluted 3-fold starting with a 1:100 dilution
515 and BAL and nasal wash samples were serially diluted 2-fold starting with a 1:2 dilution, then
516 added to the coated plates and incubated at room temperature for 2 hours. For IgG ELISA, plates
517 were washed with PBS-T, then incubated with horseradish peroxidase (HRP)-conjugated mouse
518 anti-monkey IgG (catalog number 4700-05, Southern Biotech, Birmingham, AL, USA) for 1
519 hour. For IgA ELISA, plates were washed with PBS-T and mouse anti-monkey IgA (catalog
520 number MCA2553, Bio-Rad, Hercules, CA, USA) was added for 1 hour followed by washing
521 with PBS-T, then incubation with HRP-conjugated goat anti-mouse IgG (catalog number 1030-
522 05, Southern Biotech). Plates were then developed with 3,3',5,5'-tetramethylbenzidine (TMB)
523 peroxidase substrate (Sigma, St. Louis, MO, USA). Reactions were stopped with TMB stop
524 solution (ScyTek Laboratories, Inc. Logan, UT, USA). Plates were read at OD 450 nm with a
525 SpectraMax Plus plate reader (Molecular Devices, Sunnyvale, CA, USA). EC₅₀ values and
526 endpoint titer values were calculated by 4-parameter fitting using SoftMax Pro 6.5.1 GxP
527 software. Individual animal anti-S IgG or IgA titers, and group geometric mean titer (GMT) and

Rhesus_NVX-CoV2373_rev59-AG

2 February 2021

528 95% confidence interval (95% CI) were plotted using GraphPad Prism 9.0 software. For serum
529 titers below the assay lower limit of detection (LOD), a titer of < 1000 (starting dilution) was
530 reported and a value of “50” assigned to the sample to calculate the group mean titer. For BAL
531 and nasal wash titers below the assay LOD, a titer of <2 (starting dilution) was reported and a
532 value of “1” assigned to the sample to calculate the group mean titer.

533

534 *Human angiotensin converting enzyme 2 (hACE2) receptor blocking antibody*

535 Human ACE2 receptor blocking antibody titer was determined by ELISA. Ninety-six well plates
536 were coated with 1.0 $\mu\text{g mL}^{-1}$ SARS-CoV-2 rS protein (BV2373, lot no. 16Apr20, Novavax,
537 Inc., Gaithersburg, MD, USA) overnight at 4°C. Sera were serially diluted 2-fold starting with a
538 1:20 dilution and were added to coated wells for 1 hour at room temperature. After washing, 30
539 ng mL^{-1} histidine-tagged hACE2 (Sino Biologics, Beijing, CHN) was added to wells for 1 hour
540 at room temperature. HRP-conjugated mouse anti-histidine-tag IgG (1:4000) (catalog number
541 4603-05, Southern Biotech, Birmingham, AL, USA) was added for 1 hour followed by addition
542 of TMB substrate. Plates were read at OD 450 nm with a SpectraMax Plus plate reader
543 (Molecular Devices, Sunnyvale, CA, USA) and data analyzed with SoftMax Pro 6.5.1 GxP
544 software. The % Inhibition for each dilution for each sample was calculated using the following
545 equation in the SoftMax Pro program: $100 -$
546 $[(\text{MeanResults}/\text{ControlValue}@PositiveControl)*100]$.

547

548 Serum dilution versus % Inhibition plot was generated, and curve fitting was performed by 4-
549 parameter logistic (4PL) curve fitting to data. Serum antibody titer at 50% inhibition (IC_{50}) of
550 hACE2 to SARS-CoV-2 S protein was determined in the SoftMax Pro program. The group GMT
551 and 95% CI and individual animal titers were plotted using GraphPad Prism 9.0 software. For a
552 titer below the assay lower limit of detection (LOD), a titer of < 20 (starting dilution) was
553 reported and a value of “10” assigned to the sample to calculate the group mean titer.

554

555 *SARS-CoV-2 neutralizing antibody assay*

556 The SARS-CoV-2 neutralizing antibody assay was conducted in a select agent ABSL-3
557 containment facility at the University of Maryland, School of Medicine. Sera were diluted 1:20
558 in Vero E6 cell growth media and further serially diluted 1:2 to 1:40,960. SARS-CoV-2

Rhesus_NVX-CoV2373_rev59-AG

2 February 2021

559 (multiplicity of infection (MOI) of 0.01 pfu per cell) was added to the wells for 60 min at 37°C.
560 Vero E6 media was used as a negative control. Each serum dilution was assessed
561 microscopically for inhibition of virus cytopathic effect (CPE) on Vero E6 cells. The endpoint
562 titer was reported as the reciprocal of the dilution at which 99% CPE was observed at 3 days post
563 infection^{19,54}.

564

565 *Preparation of the SARS-CoV-2 challenge stock*

566 A fourth cell-culture passage (P4) of SARS-CoV-2 isolate USA-WA1/2020 was obtained from
567 Biodefense and Emerging Infections Research Resources Repository (catalog number NR-
568 52281, BEI Resources, GenBank accession number MN985325.1). Live virus stock was
569 prepared in the Texas Biomed ABSL-3 containment facility. The stock virus was passaged for a
570 fifth time (P5) in Vero E6 cells at a MOI of 0.001 to produce the master virus stock. The master
571 stock was again passaged in Vero E6 cells at a MOI of 0.02 (P6) to produce the challenge stock.
572 The P6 challenge stock had a titer of 2.10×10^6 pfu mL⁻¹ (Lot No. 20200320) and was stored 500
573 µL aliquots at -65°C in Dulbecco's modified essential media (DMEM) and 10% fetal bovine
574 serum. The identity of the challenge stock was confirmed to be SARS-CoV-2 by deep
575 sequencing and was confirmed to be identical to the published sequence (GenBank: MN985325).

576

577 *SARS-CoV-2 challenge*

578 Vaccinated and placebo animals were transferred from the ABSL-2 facility on study day 31/32 to
579 the ABSL-3 facility and acclimated for 7 days. On the day of challenge (study day 38), animals
580 were sedated and challenged with a total target dose of 1.05×10^6 pfu in 500 µL. The challenge
581 dose was equally administered by the intranasal (IN) route 5.25×10^5 pfu in 250 µL and intra-
582 tracheal (IT) route 5.25×10^5 pfu in 250 µL. IN administration was performed with an
583 atomization device (Teleflex Intranasal Mucosal Atomization Device LMA MAD Nasal Device,
584 Morrisville, NC, USA) and IT delivery was performed with Tracheal Mucosal Atomization
585 Device (Teleflex Laryngo-Tracheal Mucosal Atomization Device LMA MADGIC, Morrisville,
586 NC, USA). To confirm the challenge dose, aliquots of the challenge samples were collected prior
587 to challenging the first animal and last animal and stored at $\leq -65^\circ\text{C}$. A neutral red agarose
588 overlay and conventional plaque assay were used to confirm the titer of the challenge dose. The
589 actual pre- and post-challenge titers were 1.80×10^6 pfu mL⁻¹ and 7.83×10^5 pfu, respectively.

Rhesus_NVX-CoV2373_rev59-AG

2 February 2021

590

591 *Sample collection for SARS-CoV-2 RNA quantification*

592 *Nasal pharyngeal swab collection.* Animals were sedated and nasal pharyngeal swabs were
593 collected prior to challenge (study day 31/32) and on 2, 3, 4, 6, and 7-8 days post infection (dpi).
594 After collection, swabs were placed in a tube containing viral transport medium (VTM), then
595 stored at $\leq -60^{\circ}\text{C}$ until processing.

596

597 *Bronchoalveolar lavage (BAL) collection.* BAL aspirates were collected prior to challenge (study
598 day 31/32) and on 2, 4 and 7-8 dpi. Animals were sedated and the trachea visualized with a
599 laryngoscope. A sterile rubber feeding tube with stylet was inserted into the trachea and into the
600 airway until it met slight resistance. Up to 80 mL of warm ($<40^{\circ}\text{C}$) sterile saline, divided into
601 multiple aliquots, was instilled through the tube. Aspirated fluid was dispensed into sterile vials
602 with VTM and stored at $\leq -60^{\circ}\text{C}$ until batch processed.

603

604 *Nasal wash collection.* Nasal washes were collected prior to infection (study day 31/32) and 2, 4,
605 and 7-8 dpi. Animals were sedated and a syringe with a flexible tipped 20-22-gauge intravenous
606 (IV) catheter was inserted into the nostril passage and a volume of 2.5-5mL of sterile saline
607 instilled. Samples were collected in sterile conical tubes containing VTM and stored at $\leq -60^{\circ}\text{C}$
608 until batch processed.

609

610 *Tissue collection.* Tissues were collected 7-8 dpi (study days 45-46) at the scheduled necropsy
611 from the upper, middle and lower lobes of the lung; nasal cavity; and trachea. Tissues were
612 weighed and stored at $80^{\circ}\text{C} \pm 10^{\circ}\text{C}$ until batch processed. RNA was extracted analyzed for the
613 presence of SARS-CoV-2 RNA via qRT-PCR targeting the N1 gene.

614

615 *Quantification of virus load in nasal swabs/washes, BAL, and tissues*

616 *Genomic (g)RNA virus.* Samples were assessed for viral load by qRT-PCR. A 250 μL aliquot of
617 VTM inactivated in TRIzol LS reagent (catalog number 10296010, ThermoFisher Scientific) was
618 used for isolation of total RNA. For total viral RNA, qRT-PCR targeting the nucleocapsid gene
619 (N1) was run on duplicate samples and results reported as genome equivalents (GE) mL^{-1} for

Rhesus_NVX-CoV2373_rev59-AG

2 February 2021

620 nasal washes/swabs and BAL. For tissue samples, results are reported as GE μg^{-1} for tissue
621 homogenates.

622 *Subgenomic (sg)RNA virus*. Replicating virus load by qRT-PCR targeting the subgenomic
623 envelope (E) gene RNA in 250 μL aliquot of nasal swabs, nasal washes, and BAL aspirates. The
624 forward and reverse primers, probe, cycling conditions, and Master Mix included:

625 SUBGEN-FORWARD: CGATCTCTTG TAGATCTGTTCTC

626 E_Sarbeco_R2 Reverse Primer: ATATTGCAGCAGTACGCACACA

627 Probe (Thermo): FAM-MGB: AACTAGCCATCCTTACTGCGCTTCG

628 TaqPath™ 1-Step RT-qPCR Master Mix, CG (catalog number A15299, ThermoFisher
629 Scientific). Cycling parameters were 25°C 2 minutes, 50°C 15 minutes, 95°C 2 minutes;
630 Amplification 40 \times 95°C 3 seconds, 60°C 30 seconds.

631 *Pseudovirus neutralizing antibody assay*.

632 SARS-CoV-2 neutralization was assessed with spike-pseudotyped virus infection of HEK
633 293T/ACE2 cells as a function of reduction in luciferase (Luc) reporter activity. HEK
634 293T/ACE2 cells were maintained in DMEM containing 10% fetal bovine serum, 25 mM
635 HEPES, 50 $\mu\text{g mL}^{-1}$ gentamycin and 3 $\mu\text{g mL}^{-1}$ puromycin. An expression plasmid encoding
636 codon-optimized full-length spike of the Wuhan-1 strain (VRC7480), was provided by Drs.
637 Barney Graham and Kizzmekia Corbett at the Vaccine Research Center, National Institutes of
638 Health (USA). The D614G amino acid change was introduced into VRC7480 by site-directed
639 mutagenesis using the QuikChange Lightning Site-Directed Mutagenesis Kit (catalog number
640 210518, Agilent Technologies). The mutation was confirmed by full-length spike gene
641 sequencing. Pseudovirions were produced in HEK 293T/17 cells (ATCC cat. no. CRL-11268,
642 Manassas, VA, USA) by transfection using Fugene 6 (catalog number E2692, Promega,
643 Madison, WI, USA) and a combination of spike plasmid, lentiviral backbone plasmid (pCMV
644 $\Delta\text{R8.2}$) and firefly Luc reporter gene plasmid (pHR' CMV Luc) in a 1:17:17 ratio⁵⁵.
645 Transfections were allowed to proceed for 16-20 hours at 37°C. Medium was removed,
646 monolayers rinsed with growth medium, and 15 mL of fresh growth medium added.
647 Pseudovirus-containing culture medium was collected after an additional 2 days of incubation
648 and was clarified of cells by low-speed centrifugation and 0.45 μm micron filtration and stored in

Rhesus_NVX-CoV2373_rev59-AG

2 February 2021

649 aliquots at -80°C. TCID₅₀ assays were performed on thawed aliquots to determine the infectious
650 dose for neutralization assays (RLU 500-1000x background, background 50-100 RLU).

651
652 For neutralization, a pre-titrated dose of virus was incubated with 8 serial 5-fold dilutions of
653 serum samples in duplicate in a total volume of 150 µL for 1 h at 37°C in 96-well flat-bottom
654 poly-L-lysine-coated Biocoat plates (catalog number 354461, Corning, NY, USA). Cells were
655 suspended using TrypLE Select Enzyme solution (Thermo Fisher Scientific) and immediately
656 added to all wells (10,000 cells in 100 µL of growth medium per well). One set of 8 control wells
657 received cells + virus (virus control) and another set of 8 wells received cells only (background
658 control). After 66-72 h of incubation, medium was removed by gentle aspiration and 30 µL of
659 Promega 1X lysis buffer was added to all wells. After a 10 minute incubation at room
660 temperature, 100 µL of Bright-Glo luciferase reagent was added to all wells. After 1-2 minutes,
661 110 µL of the cell lysate was transferred to a black/white plate (Perkin-Elmer). Luminescence
662 was measured using a PerkinElmer Life Sciences, Model Victor2 luminometer. Neutralization
663 titers are the serum dilution at which relative luminescence units (RLU) were reduced by either
664 50% (ID₅₀) compared to virus control wells after subtraction of background RLUs. Serum
665 samples were heat-inactivated for 30 min at 56°C prior to assay.

666
667 *Antibody-dependent cellular phagocytosis and neutrophil phagocytosis*

668 ADCP and ADNP were conducted as previously described^{56,57}. Briefly, NVX-CoV2373 Spike
669 protein was biotinylated using EDC (Thermo Fisher) and Sulfo-NHS (Thermo Fisher), and then
670 coupled to yellow/green Neutravidin-conjugated beads (Thermo Fisher). Immune complexes
671 were formed by incubating the bead+protein conjugates with diluted serum for 2 hours at 37°C,
672 and then washed to remove unbound antibody. The immune complexes were then incubated
673 overnight with THP-1 cells (ADCP), or for 1 hour with RBC-lyzed whole blood (ADNP). THP-1
674 cells were then washed and fixed in 4% PFA, while the RBC-lyzed whole blood was washed,
675 stained for CD66b⁺ (Biolegend) to identify neutrophils, and then fixed in 4% PFA. Flow
676 cytometry was performed to identify the percentage of quantity of beads phagocytosed by THP-1
677 cells or neutrophils, and a phagocytosis score was calculated (% cells positive × Median
678 Fluorescent Intensity of positive cells). Flow cytometry was performed with an IQue (Intellicyt)
679 or LSRII(BD) and analysis was performed using IntelliCyt ForeCyt (v8.1) or FlowJo V10.7.1.

Rhesus_NVX-CoV2373_rev59-AG

2 February 2021

680

681 *Antibody-dependent complement deposition*

682 ADCD was conducted as previously described⁵⁸. Briefly, NVX-CoV2373 Spike protein was
683 biotinylated using EDC (Thermo Fisher) and Sulfo-NHS (Thermo Fisher), and then coupled to
684 red Neutravidin-conjugated microspheres (Thermo Fisher) or directly coupled to Carboxylate-
685 Modified microspheres (Thermo Fisher). Immune complexes were formed by incubating the
686 bead+protein conjugates with diluted serum for 2 hours at 37°C, and then washed to remove
687 unbound antibody. The immune complexes were then incubated with lyophilized guinea pig
688 complement (Cedarlane) and diluted in gelatin veronal buffer with calcium and magnesium
689 (Boston Bioproducts) for 30 minutes. C3 bound to immune complexes was detected by
690 fluorescein-conjugated goat IgG fraction to guinea pig Complement Cc (MP Biomedicals). Flow
691 cytometry was performed to identify the percentage of beads with bound C3. Flow cytometry
692 was performed with an IQue (Intellicyt) and analysis was performed on IntelliCyt ForeCyt
693 (v8.1).

694

695 *Antibody-dependent NK cell degranulation*

696 Antibody-dependent NK cell degranulation was conducted as previously described⁵⁹. NVX-
697 CoV2373 Spike protein was coated on Maxisorp ELISA plate (Thermo Fisher), and then blocked
698 with 5% BSA. Antibodies were then added and incubated for 2 hours at 37°C. Human NK cells
699 were isolated from peripheral blood by negative selection using the RosetteSep Human NK cell
700 enrichment cocktail following the manufacturer's instructions. Human NK cells were then added
701 to the bound antibody and incubated for 5 hours at 37°C in the presence of RMPI+10%FBS,
702 GolgiStop (BD), Brefeldin A (Sigma), and anti-human CD107a antibody (BD Bioscience). After
703 incubation, cells were washed, stained with CD16, CD56, and CD3 (BD Bioscience), and fixed
704 in 4% PFA for 15 minutes. Intracellular staining was performed using the FIX/PERM Cell
705 fixation and permeabilization kit (Thermo), and cells were stained for interferon- γ and
706 macrophage inflammatory protein-1 β (BD bioscience). Flow cytometry was performed with an
707 IQue (Intellicyt) and analysis was performed on IntelliCyt ForeCyt (v8.1).

708

709 *Isotype and FcR-binding Luminex profiling*

Rhesus_NVX-CoV2373_rev59-AG

2 February 2021

710 Isotyping and FcR profiling was conducted as previously described^{60,61}. Briefly, antigens (NVX-
711 CoV2373 Spike, SARS-CoV-2 Spike, S1, RBD, S2, HKU-1 RBD, or OC43 RBD) were
712 carboxyl coupled to magnetic Luminex microplex carboxylated beads (Luminex Corporation)
713 using NHS-ester linkages with Sulfo-NHS and EDC (Thermo Fisher), and then incubated with
714 serum for 2 hours at 37°C. Isotyping was performed by incubating the immune complexes with
715 secondary mouse-anti-rhesus antibody detectors for each isotype (IgG1, IgG2, IgG3, IgG4, IgA),
716 then detected with tertiary anti-mouse-IgG antibodies conjugated to PE. FcR binding was
717 quantified by incubating immune complexes with biotinylated FcRs (FcγR2A-1, FcγR2A-2,
718 FcγR3A, courtesy of Duke Protein Production Facility) conjugated to Steptavidin-PE (Prozyme).
719 Flow cytometry was performed with an IQue (Intellicyt) and analysis was performed on
720 IntelliCyt ForeCyt (v8.1).

721

722 *Multivariate analysis*

723 A principal component analysis (PCA) was performed based on serological features using the R
724 package ‘ropls’. The systems serology antibody titers, FcR binding and ADCD measurements
725 were log10-transformed, and all measurements were z-scored. The PCA analyses was performed
726 in R version 4.0.2.

727

728 *Statistical analysis*

729 Statistical analyses were performed with GraphPad Prism 9.0 software. Serum antibodies were
730 plotted for individual animals and the geometric mean titer (GMT) and 95% confidence intervals
731 plotted. Virus loads were plotted as the median value, interquartile range, and minimum and
732 maximum values. Student’s t-test or two-way ANOVA was used to determine differences
733 between paired groups as indicated in the figure legends. $p \leq 0.05$ was considered significant.
734 The AUCs and bootstrap confidence intervals were calculated using the R package ‘pROC’. For
735 the case of AUC = 1 no confidence interval was provided. To visualize fold change of mutant
736 humoral features with respect to the WT, a volcano plot was constructed. To calculate p-values,
737 the R package ‘stats’ was used. The AUC and fold change analyses were performed in R version
738 4.0.2.

739

740 **Funding statement and Acknowledgements**

Rhesus_NVX-CoV2373_rev59-AG

2 February 2021

741 This work was funded by Operation Warp Speed. We thank Colin Mann and Kathryn Hastie for
742 production of Spike antigens. We thank Nancy Zimmerman, Mark and Lisa Schwartz, an
743 anonymous donor (financial support), Terry and Susan Ragon, and the SAMANA Kay MGH
744 Research Scholars award for their support. We acknowledge support from the Ragon Institute of
745 MGH, MIT and Harvard, the Massachusetts Consortium on Pathogen Readiness (MassCPR), the
746 NIH (3R37AI080289-11S1, R01AI146785, U19AI42790-01, U19AI135995-02, U19AI42790-
747 01, 1U01CA260476 – 01, CIVIC75N93019C00052), the Gates foundation Global Health
748 Vaccine Accelerator Platform funding (OPP1146996 and INV-001650), and the Musk
749 Foundation.

750

751 **Author contributions**

752 NP, MGX, YG, RC, JHT, BZ, MJM, ADP, MJG, CA, AZ, GA, CL, KMP, EOS, DL, FK, and
753 GS contributed to conceptualization of experiments, generation of data and analysis, and
754 interpretation of the results. NP, JHT, BZ, SM, YG, RC, CA, MJG, AZ, DY, KB, FA, SS, SM,
755 MEM, JL, CM, and MBF performed experiments. NP, MGX, YG, RC, GA, and MBF
756 coordinated projects. GS, GG, DL, DM, MGX, AMG, NP, YG, RC, MBF, MJG, CA, GA, CL,
757 KMP, and LE contributed to drafting and making critical revisions with the assistance of others.

758

759 **Declaration of competing interests**

760 NP, MGX, JHT, BZ, SM, AMG, MJM, ADP, GG, GS, and LE are current or past employees of
761 Novavax, Inc. and have stock options in the company. GA is the founder of SeromYx Systems,
762 Inc. AZ is a current employee of Moderna, Inc. but conducted this work before employment.
763 YG, RC, JD, EC, MG, HMS, CB, JDC, KA, MJG, CA, KMP, CL, DY, KB, MEM, JL, DM, CM,
764 SS, FA, FK, EOS, DL, and MBF declare no competing interest.

765

766

767 **References**

768

- 769 1. Dong, E., Du, H. & Gardner, L. An interactive web-based dashboard to track
770 COVID-19 in real time. *The Lancet Infectious Diseases* **20**, 533-534 (2020).
- 771 2. Huff, H.V. & Singh, A. Asymptomatic transmission during the COVID-19
772 pandemic and implications for public health strategies. *Clin Infect Dis* (2020).
- 773 3. Day, M. Covid-19: identifying and isolating asymptomatic people helped eliminate
774 virus in Italian village. *BMJ* **368**, m1165 (2020).

Rhesus_NVX-CoV2373_rev59-AG

2 February 2021

- 775 4. Meng, L., *et al.* Intubation and Ventilation amid the COVID-19 Outbreak: Wuhan's
776 Experience. *Anesthesiology* **132**, 1317-1332 (2020).
- 777 5. Polack, F.P., *et al.* Safety and Efficacy of the BNT162b2 mRNA Covid-19
778 Vaccine. *N Engl J Med* **383**, 2603-2615 (2020).
- 779 6. Jackson, L.A., *et al.* An mRNA Vaccine against SARS-CoV-2 - Preliminary
780 Report. *N Engl J Med* **383**, 1920-1931 (2020).
- 781 7. Poland, G.A., Ovsyannikova, I.G. & Kennedy, R.B. SARS-CoV-2 immunity:
782 review and applications to phase 3 vaccine candidates. *The Lancet* **396**, 1595-
783 1606 (2020).
- 784 8. Vaccines and Related Biological Products Advisory Committee Meeting.
- 785 9. UK science advisers: publish evidence behind COVID vaccine changes. *Nature*
786 **589**, 169-170 (2021).
- 787 10. Mercado, N.B., *et al.* Single-shot Ad26 vaccine protects against SARS-CoV-2 in
788 rhesus macaques. *Nature* **586**, 583-588 (2020).
- 789 11. Yu, J., *et al.* DNA vaccine protection against SARS-CoV-2 in rhesus macaques.
790 *Science* **369**, 806-811 (2020).
- 791 12. Loos, C., *et al.* Evolution of Early SARS-CoV-2 and Cross-Coronavirus Immunity.
792 *mSphere* **5**(2020).
- 793 13. Atyeo, C., *et al.* Distinct Early Serological Signatures Track with SARS-CoV-2
794 Survival. *Immunity* **53**, 524-532 e524 (2020).
- 795 14. Zohar, T., *et al.* Compromised Humoral Functional Evolution Tracks with SARS-
796 CoV-2 Mortality. *Cell* **183**, 1508-1519 e1512 (2020).
- 797 15. Nimmerjahn, F. & Ravetch, J.V. Fcγ receptors as regulators of immune
798 responses. *Nat Rev Immunol* **8**, 34-47 (2008).
- 799 16. Bournazos, S. & Ravetch, J.V. Diversification of IgG effector functions. *Int*
800 *Immunol* **29**, 303-310 (2017).
- 801 17. Bournazos, S. & Ravetch, J.V. Fcγ receptor pathways during active and
802 passive immunization. *Immunol Rev* **268**, 88-103 (2015).
- 803 18. Bournazos, S., Gupta, A. & Ravetch, J.V. The role of IgG Fc receptors in
804 antibody-dependent enhancement. *Nat Rev Immunol* **20**, 633-643 (2020).
- 805 19. Keech, C., *et al.* Phase 1-2 Trial of a SARS-CoV-2 Recombinant Spike Protein
806 Nanoparticle Vaccine. *N Engl J Med* **383**, 2320-2332 (2020).
- 807 20. Xie, X., *et al.* Neutralization of N501Y mutant SARS-CoV-2 by BNT162b2
808 vaccine-elicited sera. *bioRxiv* (2021).
- 809 21. Kupferschmidt, K. Mutant coronavirus in the United Kingdom sets off alarms, but
810 its importance remains unclear. *Science* (2020).
- 811 22. Kemp, S.A., *et al.* Neutralising antibodies in Spike mediated SARS-CoV-2
812 adaptation. *medRxiv* (2020).
- 813 23. Zhang, L., *et al.* SARS-CoV-2 spike-protein D614G mutation increases virion
814 spike density and infectivity. *Nat Commun* **11**, 6013 (2020).
- 815 24. Davies, N.G., *et al.* Estimated transmissibility and severity of novel SARS-CoV-2
816 Variant of Concern 202012/01 in England. *medRxiv* (2020).
- 817 25. Volz, E., *et al.* Transmission of SARS-CoV-2 Lineage B.1.1.7 in England: Insights
818 from linking epidemiological and genetic data. *medRxiv* (2021).

Rhesus_NVX-CoV2373_rev59-AG

2 February 2021

- 819 26. Santos, J.C. & Passos, G.A. The high infectivity of SARS-CoV-2 B.1.1.7 is
820 associated with increased interaction force between Spike-ACE2 caused by the
821 viral N501Y mutation *bioRxiv* (2021).
- 822 27. Wang, P., *et al.* Increased Resistance of SARS-CoV-2 Variants B.1.351 and
823 B.1.1.7 to Antibody Neutralization. *bioRxiv* (2021).
- 824 28. Wibmer, C.K., *et al.* SARS-CoV-2 501Y.V2 escapes neutralization by South
825 African COVID-19 donor plasma. *bioRxiv* (2021).
- 826 29. Wu, K., *et al.* mRNA-1273 vaccine induces neutralizing antibodies against spike
827 mutants from global SARS-CoV-2 variants. *bioRxiv* (2021).
- 828 30. Muik, A., *et al.* Neutralization of SARS-CoV-2 lineage B.1.1.7 pseudovirus by
829 BNT162b2 vaccine-elicited human sera. *bioRxiv* (2021).
- 830 31. Wang, Z., *et al.* mRNA vaccine-elicited antibodies to SARS-CoV-2 and circulating
831 variants. *bioRxiv* (2021).
- 832 32. Mahase, E. Covid-19: Novavax vaccine efficacy is 86% against UK variant and
833 60% against South African variant. *BMJ* (2021).
- 834 33. Callaway, E. & Mallapaty, S. Novavax offers first evidence that COVID vaccines
835 protect people against variants. *Nature* (2021).
- 836 34. Liu, Z., *et al.* Identification of SARS-CoV-2 spike mutations that attenuate
837 monoclonal and serum antibody neutralization. *Cell Host & Microbe* (2021).
- 838 35. Mahase, E. Covid-19: Pfizer vaccine efficacy was 52% after first dose and 95%
839 after second dose, paper shows. *BMJ* **371**, m4826 (2020).
- 840 36. Iwasaki, A., Foxman, E.F. & Molony, R.D. Early local immune defences in the
841 respiratory tract. *Nat Rev Immunol* **17**, 7-20 (2017).
- 842 37. Subbarao, K. & Mahanty, S. Respiratory Virus Infections: Understanding COVID-
843 19. *Immunity* **52**, 905-909 (2020).
- 844 38. Callaway, E. The coronavirus is mutating - does it matter? *Nature* **585**, 174-177
845 (2020).
- 846 39. Lee, C.Y.-P., *et al.* Neutralizing antibodies from early cases of SARS-CoV-2
847 infection offer cross-protection against the SARS-CoV-2 D614G variant. *bioRxiv*
848 (2020).
- 849 40. Plante, J.A., *et al.* Spike mutation D614G alters SARS-CoV-2 fitness. *Nature*
850 (2020).
- 851 41. Korber, B., *et al.* Tracking Changes in SARS-CoV-2 Spike: Evidence that D614G
852 Increases Infectivity of the COVID-19 Virus. *Cell* **182**, 812-827 e819 (2020).
- 853 42. Korber, B., *et al.* Spike mutation pipeline reveals the emergence of a more
854 transmissible form of SARS-CoV-2. *bioRxiv* (2020).
- 855 43. Weissman, D., *et al.* D614G Spike Mutation Increases SARS CoV-2
856 Susceptibility to Neutralization. *Cell Host Microbe* **29**, 23-31 e24 (2021).
- 857 44. Starr, T.N., *et al.* Deep Mutational Scanning of SARS-CoV-2 Receptor Binding
858 Domain Reveals Constraints on Folding and ACE2 Binding. *Cell* **182**, 1295-1310
859 e1220 (2020).
- 860 45. Tegally, H., *et al.* Emergence and rapid spread of a new severe acute respiratory
861 syndrome-related coronavirus 2 (SARS-CoV-2) lineage with multiple spike
862 mutations in South Africa. *medRxiv* (2020).
- 863 46. Mahase, E. Covid-19: What have we learnt about the new variant in the UK?
864 *BMJ* **371**, m4944 (2020).

Rhesus_NVX-CoV2373_rev59-AG

2 February 2021

- 865 47. Voloch, C.M., *et al.* Genomic characterization of a novel SARS-CoV-2 lineage
866 from Rio de Janeiro, Brazil. *medRxiv* (2020).
- 867 48. Greaney, A.J., *et al.* Complete Mapping of Mutations to the SARS-CoV-2 Spike
868 Receptor-Binding Domain that Escape Antibody Recognition. *Cell Host Microbe*
869 **29**, 44-57 e49 (2021).
- 870 49. Weisblum, Y., *et al.* Escape from neutralizing antibodies by SARS-CoV-2 spike
871 protein variants. *Elife* **9**(2020).
- 872 50. Corey, L., Mascola, J.R., Fauci, A.S. & Collins, F.S. A strategic approach to
873 COVID-19 vaccine R&D. *Science* **368**, 948-950 (2020).
- 874 51. Hodgson, S.H., *et al.* What defines an efficacious COVID-19 vaccine? A review
875 of the challenges assessing the clinical efficacy of vaccines against SARS-CoV-
876 2. *The Lancet Infectious Diseases* (2020).
- 877 52. Lovgren, K. & Morein, B. The requirement of lipids for the formation of
878 immunostimulating complexes (iscoms). *Biotechnol Appl Biochem* **10**, 161-172
879 (1988).
- 880 53. Wrapp, D., *et al.* Cryo-EM structure of the 2019-nCoV spike in the prefusion
881 conformation. *Science* **367**, 1260-1263 (2020).
- 882 54. Tian, J.-H., *et al.* SARS-CoV-2 spike glycoprotein vaccine candidate NVX-
883 CoV2373 elicits immunogenicity in baboons and protection in mice. *bioRxiv*
884 (2020).
- 885 55. Naldini, L., Blomer, U., Gage, F.H., Trono, D. & Verma, I.M. Efficient transfer,
886 integration, and sustained long-term expression of the transgene in adult rat
887 brains injected with a lentiviral vector. *Proc Natl Acad Sci U S A* **93**, 11382-11388
888 (1996).
- 889 56. Butler, A.L., Fallon, J.K. & Alter, G. A Sample-Sparing Multiplexed ADCP Assay.
890 *Front Immunol* **10**, 1851 (2019).
- 891 57. Karsten, C.B., *et al.* A versatile high-throughput assay to characterize antibody-
892 mediated neutrophil phagocytosis. *J Immunol Methods* **471**, 46-56 (2019).
- 893 58. Fischinger, S., *et al.* A high-throughput, bead-based, antigen-specific assay to
894 assess the ability of antibodies to induce complement activation. *J Immunol*
895 *Methods* **473**, 112630 (2019).
- 896 59. Gunn, B.M., *et al.* A Role for Fc Function in Therapeutic Monoclonal Antibody-
897 Mediated Protection against Ebola Virus. *Cell Host Microbe* **24**, 221-233 e225
898 (2018).
- 899 60. Brown, E.P., *et al.* High-throughput, multiplexed IgG subclassing of antigen-
900 specific antibodies from clinical samples. *J Immunol Methods* **386**, 117-123
901 (2012).
- 902 61. Brown, E.P., *et al.* Multiplexed Fc array for evaluation of antigen-specific antibody
903 effector profiles. *J Immunol Methods* **443**, 33-44 (2017).

904

Rhesus_NVX-CoV2373_rev59-AG

2 February 2021

905 **Figure Legends**

906

907 **Figure 1. Subgenomic RNA and viral RNA in upper and lower respiratory tract of NVX-**
908 **CoV2373 immunized rhesus macaques**

909 (A) Groups of adult rhesus macaques (n= 4-5/group) were immunized with a single priming dose
910 (study day 0) or a prime/boost regimen (study day 0 and 21) of 5 µg or 25 µg NVX-CoV2373
911 with 50 µg Matrix-M (0.5mL; IM). A separate group (n=4) received formulation buffer
912 (placebo). Immunized and placebo animals were transferred to an ABSL-3 containment facility
913 (study day 31/32) and acclimated for 7 days prior to challenge with a total of 1.05×10^6 pfu
914 SARS-CoV-2 (USA-WA1/2020 isolate) in 500 µL divided between the intranasal (IN) and intra-
915 tracheal (IT) routes. Animals were monitored daily for up to 7-8 days post infection (1-8 dpi).
916 Serum sample collection days are indicated by the red triangles. Bronchoalveolar lavage (BAL)
917 sample collection days are indicated by the blue triangles. Necropsy and tissue collection is
918 indicated by the black triangle. Quantitative RT-PCR was used to measure the replicating
919 subgenomic (sg) envelope (E) RNA in nasal washes, nasal pharyngeal swabs, and BAL samples
920 collected for up to 7-8 dpi. (B) Nasal pharyngeal washes. (C) Nasal swabs. (D) BAL aspirates.
921 (E) SARS-CoV-2 gRNA in the Nasal cavity virus load. (F) Trachea virus load. (G) Upper,
922 middle and lower lobes of the lungs of immunized and placebo treated animals. In the bar-and-
923 whisker plots, the median is indicated by a horizontal line, the top and bottom of the box
924 indicated the interquartile range, and the whiskers indicate the minimum and maximum values.
925 Individual animal values are indicated by the colored symbols. Dashed horizontal line indicates
926 the limit of detection. Genomic equivalent copies (GE copies mL⁻¹). Significant differences
927 between the placebo group and the immunized groups was determined by Student's t-test (two
928 tailed, unpaired). Not significant (ns), *p ≤ 0.05, **p ≤ 0.01, ***p ≤ 0.001, ****p ≤ 0.0001.

929

930 **Figure 2. Immunogenicity of NVX-CoV2373 vaccine in rhesus macaques**

931 (A) Serum anti-S IgG titer (B) Nasal wash and (C) bronchoalveolar lavage (BAL) samples were
932 collected 31/32 days after the first immunization and prior to challenge and analyzed for spike
933 (S)-specific mucosal IgG (n= 4-5/group). (D) Pseudovirus neutralizing titer (ID₅₀). (E) SARS-
934 CoV-2 neutralizing antibody titer (99% inhibition of cytopathic effect, 99% CPE) study day
935 31/32. (F) hACE2 receptor blocking antibody titer (study day 31/32). The geometric mean titers
936 (GMT) are indicated by the white bars. Hollow arrows indicate prime/boosting with NVX-
937 CoV2373. The error bars indicate the 95% confidence interval (95% CI). Individual animal
938 values are indicated by colored symbols. A Student's t-test (unpaired, two tail) was used to
939 compare antibody levels between groups immunized with one and two doses. **p ≤ 0.001, ***p
940 ≤ 0.0001, ****p ≤ 0.00001. The horizontal dashed line indicates the limit of detection (LOD) for
941 each assay.

942

943 **Figure 3. System serology profiling of NVX-CoV2373 immunized rhesus macaques**

944 Serum was collected day 21 and day 31/32 after the first dose of NVX-CoV2373, and profiled
945 for the anti-NVX-CoV2373 antibody response. Luminex was used to quantify the (A) antibody
946 isotypes (IgG1, IgA, and IgM) and (B) FcR binding (FcγRIIA-1, FcγRIIA-2, FcγRIIIA) for the
947 anti-NVX-CoV2373 antibody response. (C) The functional anti-NVX-CoV2373-specific
948 antibody responses for antibody-dependent cellular phagocytosis, antibody-dependent neutrophil
949 phagocytosis, antibody-dependent complement deposition, and antibody-dependent NK
950 degranulation (measured by CD107%). A two-way ANOVA with Tukey correction for multiple

Rhesus_NVX-CoV2373_rev59-AG

2 February 2021

951 comparison was used to compare antibody levels between groups. Not significant (ns), * $p \leq 0.05$,
952 ** $p \leq 0.01$, *** $p \leq 0.001$, **** $p \leq 0.0001$.

953

954 **Figure 4. Unique humoral profile of vaccine regimens**

955 Multivariate analysis was performed to distinguish the humoral response between the various
956 vaccine regimens. (A) Heatmap of the humoral response to SARS-CoV-2 spike. Each Column is
957 one NHP and one time point. Each row was Z-scored across itself for the whole cohort. (B)
958 Principal component analysis (PCA) of antibody features at day 31/32 showing NHPs that
959 received one 5 μ g dose (light blue) or one 25 μ g dose (dark blue). Ellipses indicate 90%
960 confidence regions assuming a multivariate t distribution. (C) PCA of antibody features at day
961 31/32 showing NHPs that received two 5 μ g doses (light pink) or two 25 μ g doses (dark pink). (D)
962 PCA of antibody features at day 31/32 showing NHPs that received one 5 μ g dose (light pink),
963 one 25 μ g dose (dark pink), two 5 μ g doses (light blue), or two 25 μ g doses (dark blue). (E) The
964 radar plots show the median percentile for antibody titer, FcR binding, and antibody function
965 (legend on right) for NHPs treated with placebo, two 5 μ g doses, two 25 μ g doses, one 5 μ g dose,
966 or one 25 μ g dose in serum collected on day 21 (top row) and day 31/32 (bottom row).

967

968 **Figure 5. Immune correlates of protection from viral replication**

969 Multivariate analysis was performed to identify the features of a protective humoral response.
970 (A) Principal component analysis (PCA) for the immunized NHPs (n=20, no placebos included)
971 indicating protected (blue) NHPs with no detectable virus in BAL, BAL + nasal swab, BAL +
972 nasal swab + nasal wash vs non-protected (yellow) NHPs. Ellipses indicate 90% confidence
973 regions assuming a multivariate t distribution and are shown for protected and non-protected
974 NHPs. (B) Correlates of protection for BAL (n=20), nasal swab (n=20), or nasal wash (n=19) at
975 day 31/32. The area-under-the-curve (AUC) for the receiver operator characteristic (ROC) curve
976 is shown with 95% confidence intervals for each antibody feature. (C) The radar plots show the
977 median percentile for antibody titer, FcR binding, and antibody function (legend on right) for
978 non-protected, protected in BAL, protected in BAL+nasal swab, or protected in BAL+nasal
979 swab+nasal wash NHPs.

980

981 **Figure 6. Antibody binding and functionality against emerging SARS-CoV-2 variant spike** 982 **proteins**

983 (A) NHP Serum (n=24) was collected day 31/32 after the first dose of NVX-CoV2373, and
984 profiled for the antibody response to the emerging SARS-CoV-2 variants, N501Y Δ 69-70 Spike,
985 E484 Spike, B.1.1.7 RBD, B.1.351 RBD, and E484K RBD. Luminex was used to quantify and
986 correlate the antibody isotypes (IgG1 and IgG3) and FcR binding (Fc γ RIIA-1 and Fc γ RIIIA)
987 response between WT Spike protein and SARS-CoV-2 variants Spike or RBD proteins. (B)
988 Serum was collected after vaccinations from individuals (n=237) vaccinated with NVX-
989 CoV2373, and the antibody response was profiled. Luminex was used to quantify and correlated
990 antibody isotypes (IgG1) and FcR binding (Fc γ RIIA and Fc γ RIIIA). PCA plots show the
991 multivariate distribution of the antibody profiles across all macaques (C) and humans (D) for
992 Spike (left) or RBD (right) humoral immune responses. The color of the dots represents the sum
993 of the scaled magnitude of the labeled Spike (left) or RBD (right) variant humoral immune
994 response.

995

996 **Supplementary Figure 1. Gating strategy for flow cytometry**

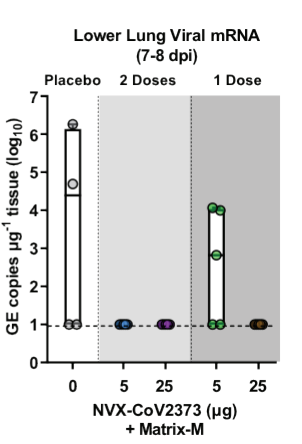
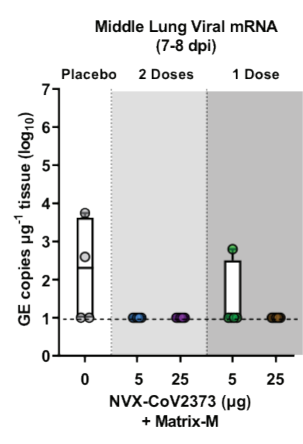
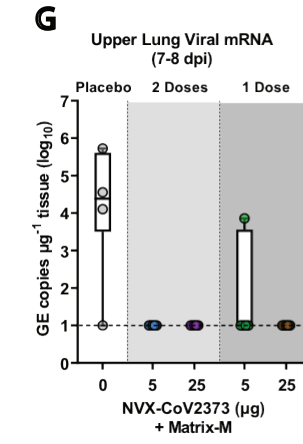
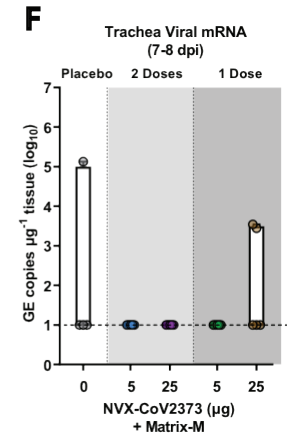
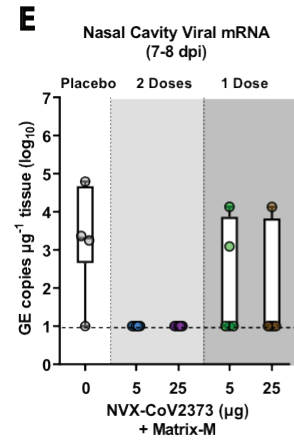
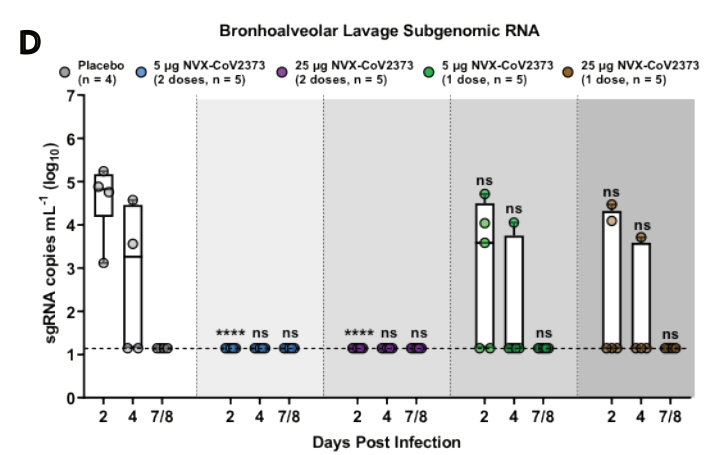
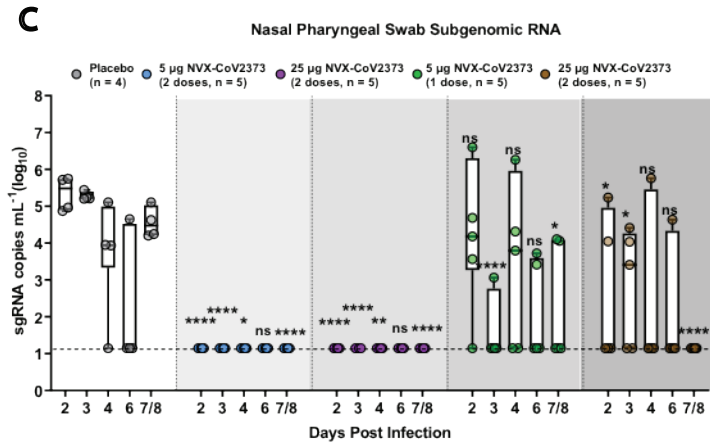
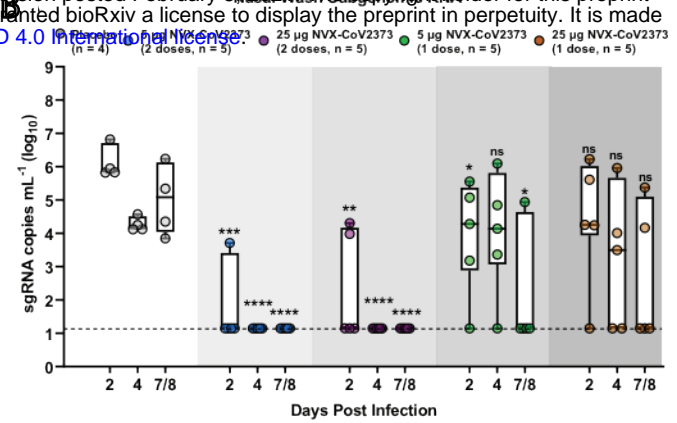
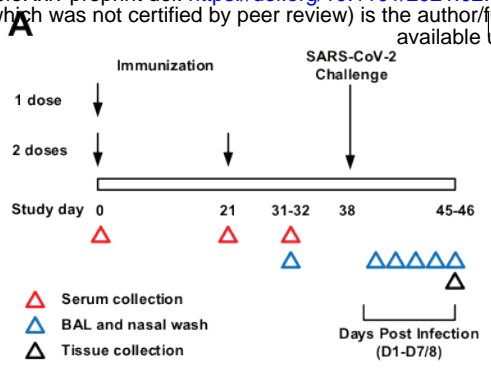
Rhesus_NVX-CoV2373_rev59-AG

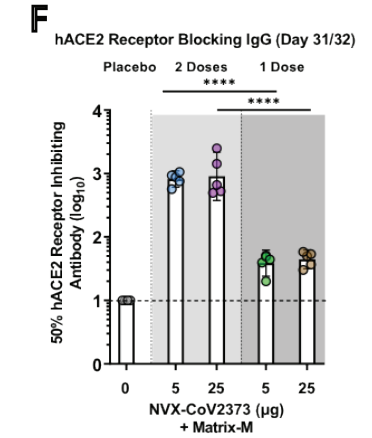
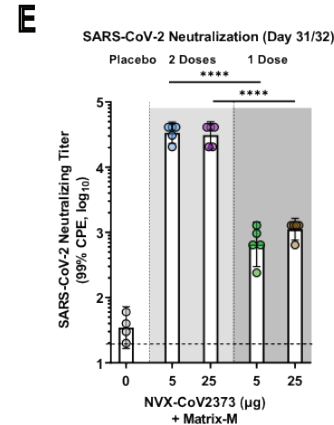
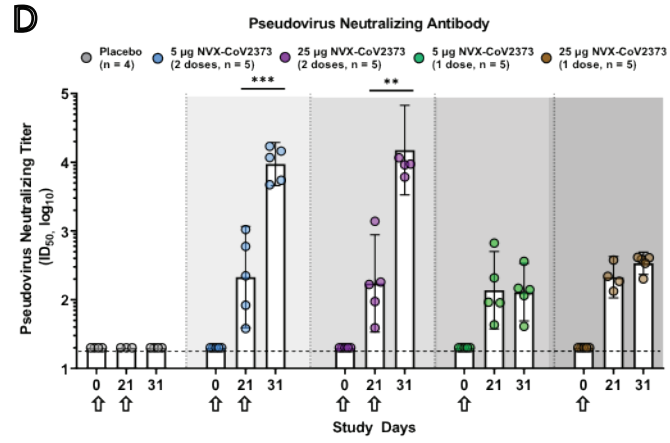
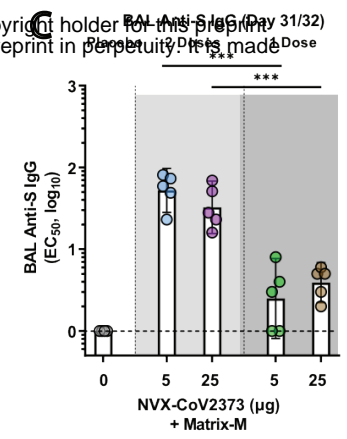
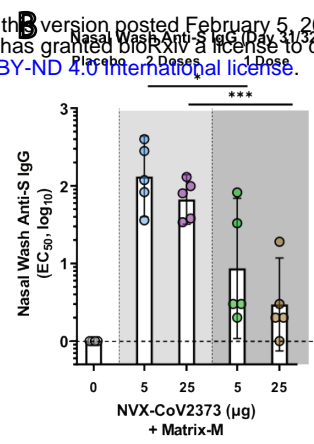
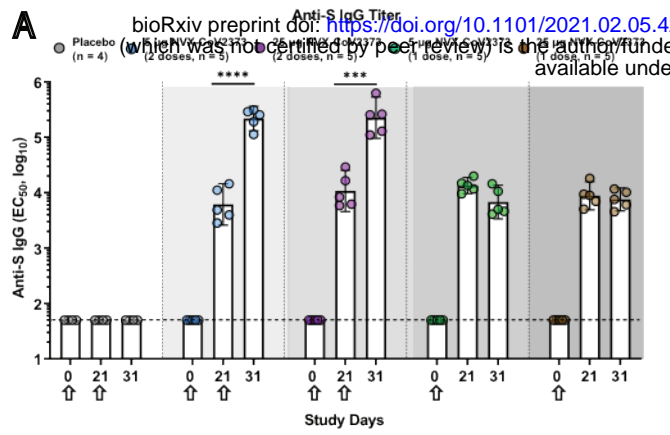
2 February 2021

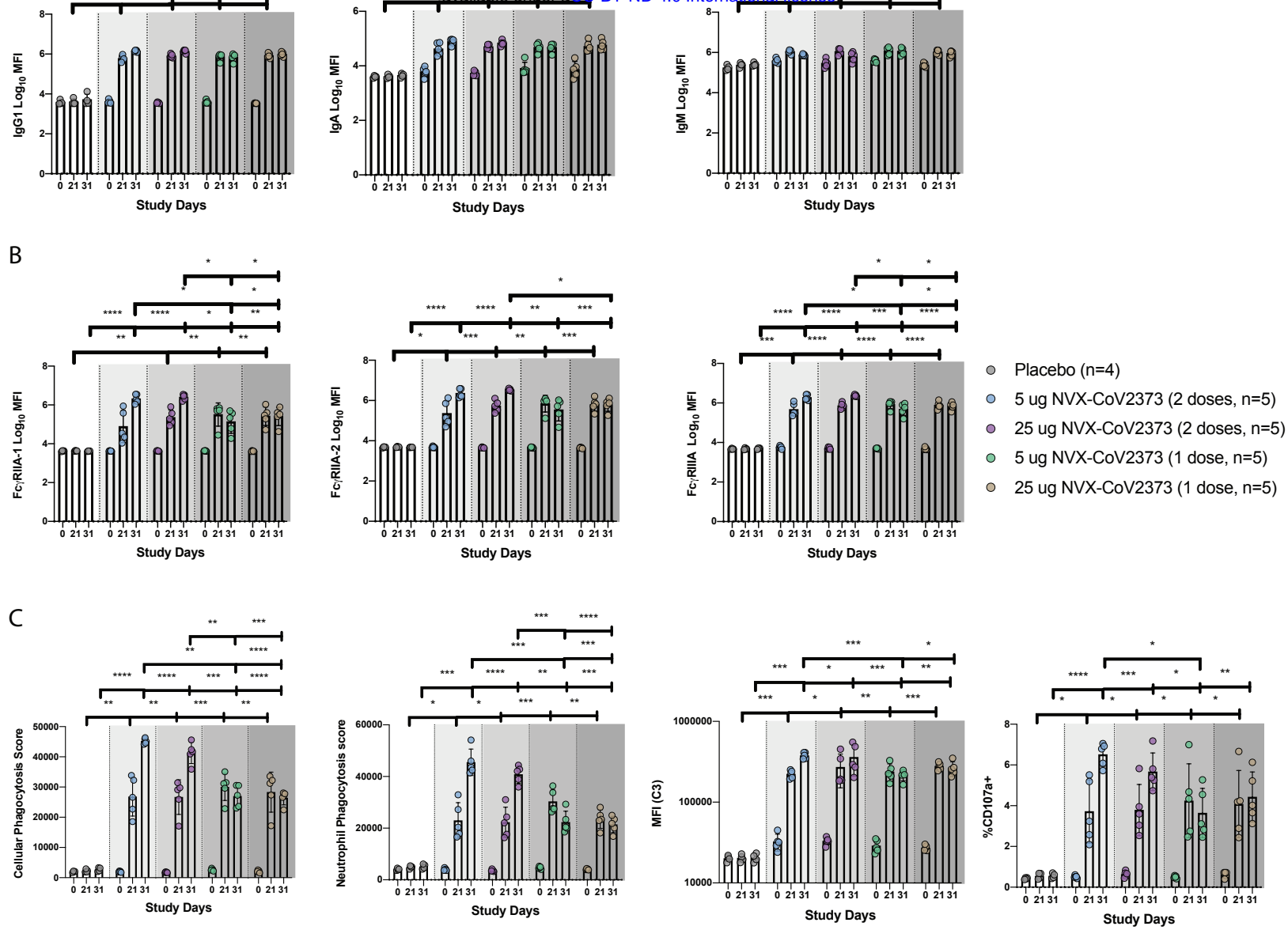
997 Example of flow cytometry gating scheme for (A) antibody-dependent cellular phagocytosis
998 (ADCP), (B) antibody-dependent neutrophil phagocytosis (ADNP), (C) antibody-dependent
999 complement deposition (ADCD), and (D) antibody-dependent NK degranulation (measured by
1000 CD107%) (NKdegran).
1001

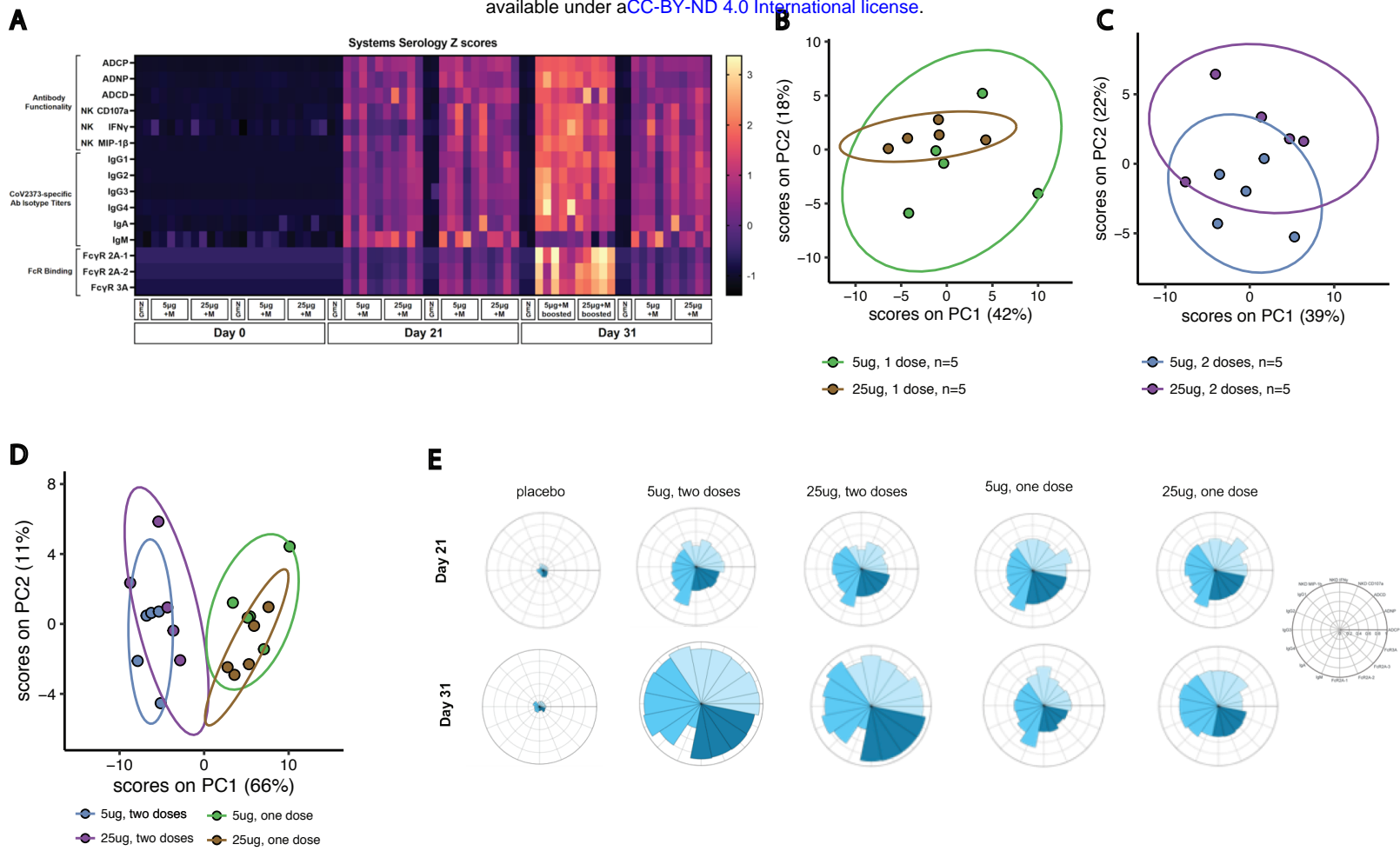
1002 **Supplementary Figure 2. Antibody and FcR binding against emerging SARS-CoV-2**
1003 **variant spike proteins**

1004 (A) Loadings plot for PC 2 of the NHP PCA model in Figure 6. Features are colored by variant
1005 protein. (B) Loadings plot for PC 2 of the Human PCA model in Figure 6. Features are colored
1006 by variant protein. (C) Volcano plot of each humoral feature for the immunized NHPs. The fold
1007 change in respect to the D614G Spike for spike features or WT RBD for RBD features is plotted
1008 in the volcano plot. (B) Volcano plot of each humoral feature for the vaccinated individuals. The
1009 fold change in respect to the D614G Spike for spike features or WT RBD for RBD features is
1010 plotted in the volcano plot.
1011



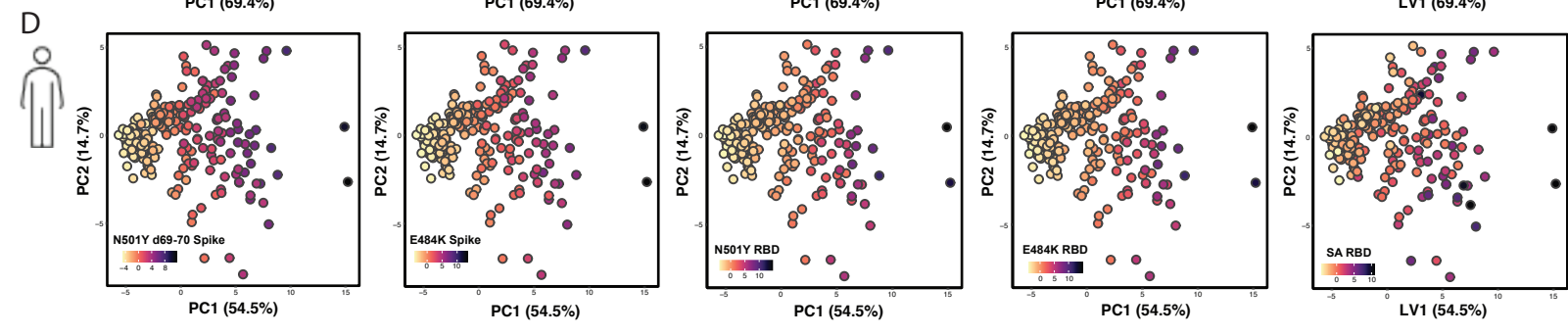
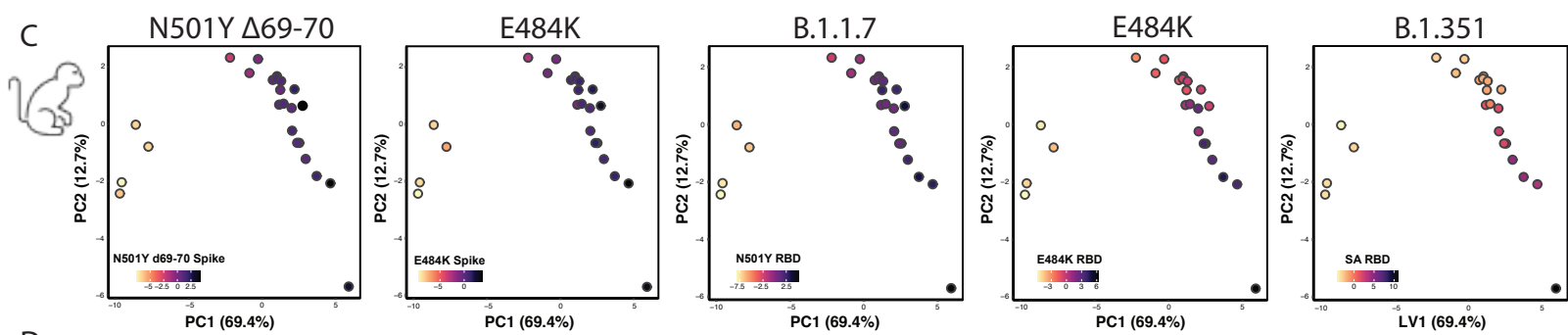
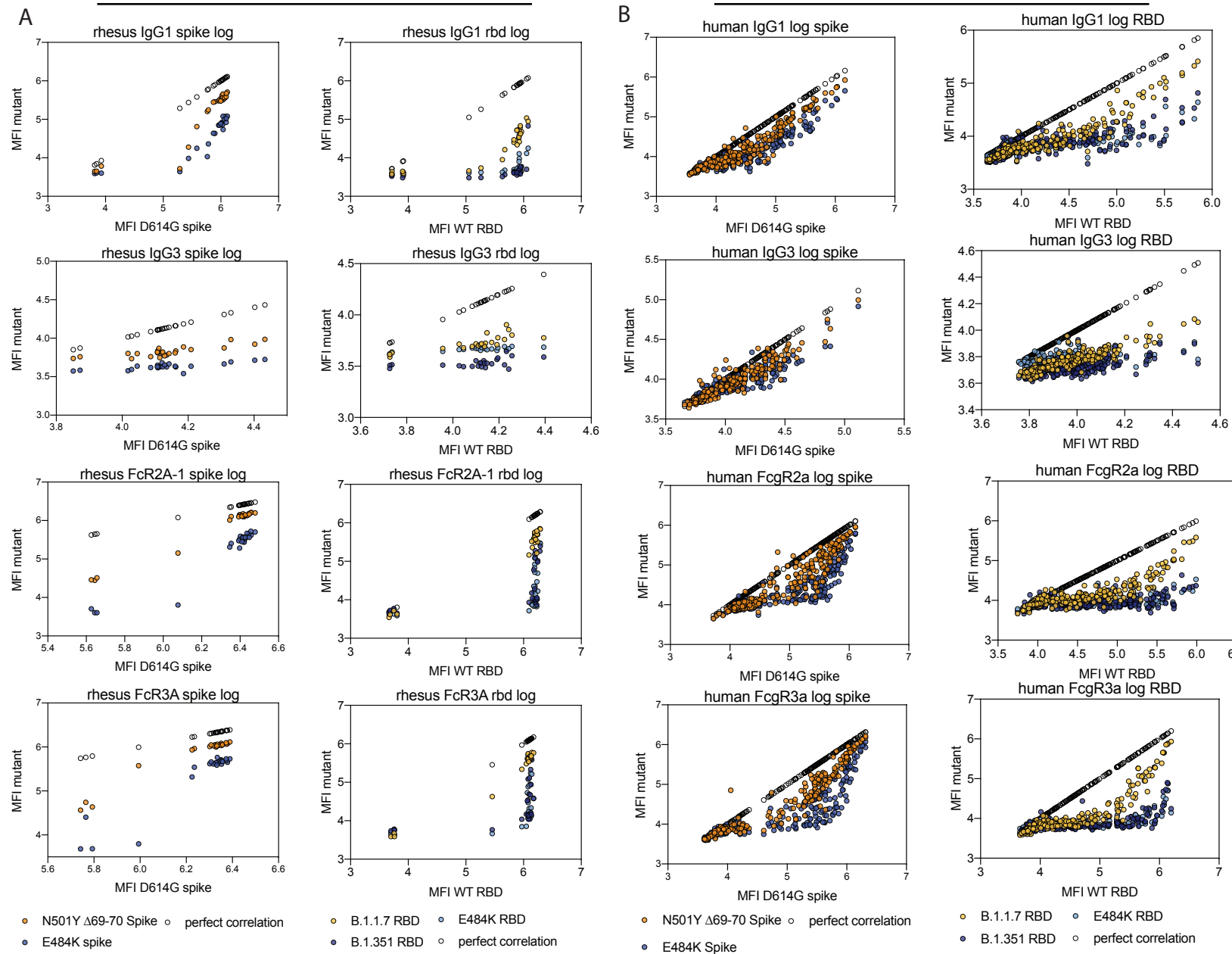






Macaques

Human



Spike

RBD